ECONOMIC RESEARCH
FEDERAL RESERVE BANK OF ST. LOUIS

WORKING PAPER SERIES

Testing for Multi-Asset Systemic Tail Risk

Authors	Deniz Erdemlioglu, Christopher J. Neely, and Xiye Yang
Working Paper Number	2023-016D
Revision Date	September 2025
Citable Link	https://doi.org/10.20955/wp.2023.016
Suggested Citation	Erdemlioglu, D., Neely, C.J., Yang, X., 2025; Testing for Multi-Asset Systemic Tail Risk, Federal Reserve Bank of St. Louis Working Paper 2023-016. URL https://doi.org/10.20955/wp.2023.016

Federal Reserve Bank of St. Louis, Research Division, P.O. Box 442, St. Louis, MO 63166

The views expressed in this paper are those of the author(s) and do not necessarily reflect the views of the Federal Reserve System, the Board of Governors, or the regional Federal Reserve Banks. Federal Reserve Bank of St. Louis Working Papers are preliminary materials circulated to stimulate discussion and critical comment.

Testing for Multi-Asset Systemic Tail Risk*

Deniz Erdemlioglu
Department of Finance, IESEG School of Management and CNRS

Christopher J. Neely
Research Division, Federal Reserve Bank of St. Louis

Xiye Yang
Department of Economics, Rutgers University

September 9, 2025

Abstract

We develop a testing framework to measure market-wide (systemic) tail risk in the cross-section of asset returns. Using high-frequency data on individual U.S. stocks and sector-specific ETF portfolios, we estimate time-varying jump intensities and test for multi-asset tail risk around Fed policy announcements. The magnitude of the tail risk induced by Fed policy announcements varies over the business cycle, peaks during the global financial crisis, and remains high during phases of unconventional monetary policy. While most FOMC announcements generate systemic left-tail risk, there is no evidence that macro announcements have a similar effect. We use our approach to construct a Fed-driven systemic tail risk (STR) indicator. STR helps explain the pre-FOMC announcement drift and significantly increases variance risk premia, particularly for the meetings without press conferences. Our measure complements existing option-based tail risk measures in identifying tail events.

Keywords: Time-varying tail risk, High-frequency data, FOMC news, Monetary policy announcements, Cojumps, Systemic risk, Jump intensity

JEL: C12, C14, C22, C32, C58, G12, G14

*We thank Olivier Scaillet, John Maheu, Stephen Roberts, Gustavo Schwenkler, as well as seminar and conference participants at the MFA Conference (2024), DeGroote School of Business, McMaster University (2021), Oxford-Man Institute of Quantitative Finance (2021), 13th Annual SoFiE conference (2021), NBER-NSF Time Series Conference (2021), Federal Reserve Bank of St. Louis (2021), OCC Symposium on Systemic Risk and Stress Testing in Banking (2022) for valuable comments and suggestions. We are also grateful to Viktor Todorov and Fabian Hollstein for sharing their data on left-tail risk measures. We thank Nancy R. Xu for excellent suggestions and discussion on an earlier version of this paper. The views expressed are those of the individual authors and do not necessarily reflect official positions of the Federal Reserve Bank of St. Louis, the Federal Reserve System, or the Board of Governors.

1 Introduction

Tail events produce large financial losses during market downturns. The crash of "Black Monday" (October 19, 1987), the TARP rejection of the U.S. House of Representatives (September 29, 2008), the Flash Crash (May 6, 2010) and Covid-19 events (e.g., March 16, 2020) are examples of abnormal equity volatility coupled with big price drops or jumps.

While Merton (1976) suggests that investors can mitigate such *idiosyncratic* jump risks through diversification strategies, recent studies have challenged this conventional wisdom. For instance, Bégin et al. (2020) show that idiosyncratic jump risk is priced in options and it helps explain excess equity returns. Studies with high frequency data also support the presence of *systematic* cojump risk. Pelger (2020), Bollerslev et al. (2008) and Bollerslev et al. (2013) provide strong evidence of systematic cojump risk embedded in the cross-section of high-frequency returns. Other related works include jump dependence tests (Bollerslev et al., 2013), cross-sectional assessments (Bibinger et al., 2019; Chan et al., 2017), and risk diversification analyses (Gilder et al., 2014; Bollerslev et al., 2008; Todorov and Bollerslev, 2010), among others.[1]

In this paper, we argue that bifurcating jumps into idiosyncratic or systematic classes is too restrictive to adequately characterize *systemic* risk. Idiosyncratic jumps occur in a single security (i.e., when $N = 1$) while systematic cojumps refer to instances in which a stock cojumps with the market index. In line with Caporin et al. (2017), Das and Uppal (2005), these two forms of jumps likely overlook the magnitude of system-wise tail risk embedded in many assets but not the entire market (i.e., when $N >> 2$). Even if an investor is able to diversify the risk attributed to idiosyncratic or systematic jumps, there is no guarantee that a strategy based on $N = 1$ or $N = 2$ will also work when many assets jump.[2] Systemic cojumps and synchronized multi-asset crashes (i.e., *downward cojumps*) could create heavier tail risk than that associated with idiosyncratic or systematic jumps.

[1] The literature on cojumps is considerably large and covers the cases beyond those only between individual assets and aggregated market index. In this direction, see also Bandi and Renò (2016), Jacod and Todorov (2009), Jacod and Todorov (2010), Todorov and Tauchen (2011) and Jacod et al. (2017), who study cojumps between jumps in prices and jumps in volatility process. Further, a large number of studies detect the arrivals of cojumps across different asset classes and markets, see e.g., Lahaye et al. (2011), Evans (2011), Dungey and Hvozdyk (2012), Winkelmann et al. (2016), Bibinger and Winkelmann (2015), Corradi et al. (2020) and Aït-Sahalia and Xiu (2016).

[2] Consider stocks, for example. If the volatility or price of an individual stock jumps, then a trader may mitigate the realized risk exposure—triggered by the jump—through dynamic asset allocation. This is possible by treating the detected jumps as risk signals and rebalancing the position as soon as a large jump occurs. In another scenario when a stock price jumps simultaneously with the market index (or another stock), investors can protect against the market (jump) risk by diversifying through sector rotation. The equity jump risk that is attributed to one specific sector (including, for instance, cyclical stocks) can be offset by shifting the allocation towards defensive sectors (such as healthcare or utilities).

In the spirit of Das and Uppal (2005) and Caporin et al. (2017), we define systemic risk as the simultaneous occurrence of jumps in multiple financial assets. Consistent with the direction of Das and Uppal (2005) and Caporin et al. (2017), we thus conjecture that systemic cojumps drive synchronized (multi-asset) systemic risk. In contrast with these two studies, however, we condition on news to identify systemic risk and we do so by exploiting the tail component of the asset price jumps. News from Federal Open Market Committee (FOMC) meetings is typically associated with prolonged trading intensity, volatility and extreme price changes (see Bollerslev et al., 2018; Weller, 2019).[3] We develop a methodology to quantify news-driven cojumps and assess which events create systemic reaction and tail risk, which permits policy-makers to identify systemically important news events.

Our econometric approach, which nests existing jump tests, builds on and extends the conditional testing approach of Erdemlioglu and Yang (2022) to a multivariate cross-sectional setting.[4] By conditioning on event times, we first estimate time-varying jump intensities that capture the tails of return distributions. We then identify news-induced systemic cojumps, controlling for the multiple testing bias. Finally, we quantify the associated right and left tail risk by using positive and negative high-frequency returns, respectively. We examine which events trigger systemic (downside) risk and how frequently these tail risk episodes occur in the marketplace.

Our application to Dow Jones stocks and sector specific exchange-traded funds (ETFs) shows that FOMC news creates systemic tail risk. We identify many instances in which almost all individual stocks and sector ETFs crash together after FOMC news. These Fed-driven systemic common jumps across individual stocks and sector portfolios impede diversification. The tail risk from these systemic cojumps and crashes reflects the market's sensitivity to policy announcements. This downside sensitivity varies over time and is closely linked to quantitative easing.

We explore the implications of Fed-driven systemic tail risk: First, we revisit the pre-FOMC drift

[3]FOMC statements potentially reveal insights to the public regarding the monetary policy reaction function and its implementation. The news conveys important signals about the FOMC's projection for macroeconomic conditions in the future (see Cieslak and Schrimpf, 2019; Nakamura and Steinsson, 2018). The literature exploring the financial effects of FOMC and monetary policy news typically conducts high-frequency event studies (see e.g., Cieslak and Schrimpf, 2019; Neely, 2015; Bauer and Neely, 2014; Gagnon et al., 2011; Joyce et al., 2011). Hattori et al. (2016) conduct event study regressions to assess the impact of unconventional Fed policy on equity market tail risk. Our event-driven high-frequency approach hence aligns with the perspective taken in such studies. See also Fratzscher et al. (2018), who classify the Fed's monetary policy events, such as large-scale asset purchase (LSAP) announcements.

[4]Important studies on univariate jumps include Lee and Hannig (2010), Lee and Mykland (2008), Lee (2012) Andersen et al. (2007), and Barndorff-Nielsen and Shepard (2006), Aït-Sahalia and Jacod (2009b), among others. Furthermore, see Dumitru and Urga (2012) and Maneesoonthorn et al. (2020), who compare different jump tests and provide excellent surveys on jump studies.

puzzle (Lucca and Moench, 2015) and find that FOMC-driven systemic tail risk may help explain *one meeting ahead* pre-FOMC announcement returns. Second, we show that Fed-driven systemic tail risk is priced in the option market: systemic tail risk significantly increases variance risk premia around FOMC announcements without a press conference. Investors and market participants seem to demand compensation to bear the systemic tail risk embedded in the cross-section of U.S. equities. There is no evidence that macroeconomic news announcements create systemic tail risk, however. This finding strongly supports the conclusions documented in Bajgrowicz et al. (2016) on the link between macro news and jump/cojump risks: Macro news could trigger sharp changes in volatility that could be mistaken for jumps or cojumps.

The rest of the paper is organized as follows. The next section discusses the contribution of our paper to the literature. Section 3 outlines the underlying model and presents our strategy to identify the news-induced systemic tail risk. Section 4 introduces the estimation approach and detection procedures. Section 5 presents our Monte Carlo study. Sections 6 and 7 describe the data and present our empirical analysis, respectively. Section 8 reports robustness checks and Section 9 concludes. The Supplementary Appendix collects all proofs, technical results, and additional analyses.

2 Related Literature

Compared to research on *idiosyncratic* and *systematic* jump risks (see e.g., Bégin et al., 2020; Pelger, 2020; Chan et al., 2017; Bollerslev et al., 2013, 2008), there is relatively little research on *systemic* cojump risk. Among these latter studies, Das and Uppal (2005) identify systemic cojump risk in a jump-diffusion setting and investigate portfolio implications at monthly trading scales. The authors find weak evidence of systemic cojump risk with an international asset allocation exercise. In contrast, our high-frequency analysis reveals strong evidence of systemic cojump (tail) risk in the cross-section of stocks. Caporin et al. (2017) make a notable contribution in detecting systemic cojumps at high frequency.

We complement and extend Caporin et al. (2017) in several respects. First, we detect *intradaily* systemic cojumps whereas Caporin et al. (2017) propose a *daily* test. Second, we condition on event timing, which permits accurate quantification of the marketwide risk. Third, our time-varying jump intensity specification is consistent with the regularities found by Bates (2019) and Andersen et al. (2020). These extensions matter: we find more severe systemic risk exposure in the intradaily jumps than do

Caporin et al. (2017) with a daily test.

Our paper is also related to studies that measure tail risk using financial data (e.g., Andersen et al., 2020; Weller, 2019; Van Oordt and Zhou, 2016; Bollerslev and Todorov, 2014 and Bollerslev et al., 2013). For example, Bollerslev et al. (2013) exploit jump tails and characterize extreme dependencies among high-frequency stock returns. In a market microstructure setup, Weller (2019) extends the framework of Bollerslev and Todorov (2014) to examine tail risk at high frequency. Van Oordt and Zhou (2016) use low-frequency (daily and monthly) data and estimate tail betas in the cross-section of stock returns. Comparing various tail risk measures, Dierkes et al. (2024) document that the option-implied tail risk measure of Bollerslev and Todorov (2011) ($BT11Q$) performs best in predicting tail risk.

Our objectives and methods differ from those of these tail-risk studies in several important respects. First, we identify *systemic* (multiple asset) tail risk while these works measure *systematic* (pairwise) tail risk, that is, risk of cojumping with the market index. Second, we follow Andersen et al. (2020), Erdemlioglu and Yang (2022) and use time-varying jump intensities to measure systemic downside risk. Third, we measure tail risk *simultaneously* across stocks, conditional on the release times of news events that alter jump intensities. Unlike Van Oordt and Zhou (2016) who gauge *systematic* tail risk by using daily and monthly data, we use jump activity index based on high-frequency data to quantify *systemic* tail risk. Finally, we compare our ranking of tail risk events with the ranking generated by the $BT11Q$ approach along with the left tail risk measures of Bollerslev et al. (2015); Andersen et al. (2021) and Todorov and Zhang (2022). We document a close relationship with $BT11Q$ approach, which implies that our approach is prone to *measurement error*, as Dierkes et al. (2024) consider measurement error to be the main driver of the relative performance of tail risk measures. Our systemic tail risk measure complements these existing tail risk measures by being adaptable to different contexts (e.g., asset classes, regions, or time horizons) and easy to compute, requiring only high-frequency data and event time stamps.

Our findings also shed light on a recent debate in this literature that asks whether news truly creates jumps or just the appearance of jumps through changes in volatility. Lahaye et al. (2011) and Amengual and Xiu (2018), respectively, find evidence that price jumps and volatility jumps occur due to FOMC news surprises. In sharp contrast, Bajgrowicz et al. (2016) argue that most detected intradaily jumps are spurious due to multiple testing bias and that news announcements tend to create *volatility bursts*, but not price jumps. We resolve this debate with the event-based extension of Romano and Wolf (2005)' StepM

bias correction. This procedure replaces traditional (and typically ad hoc) jump-news matching methods. Our approach suggests that jumps are strongly associated with FOMC announcements, but there is no clear evidence that macroeconomic news creates *real* (i.e., non-spurious) systemic cojumps. Therefore, tail risk due to macro news is potentially diversifiable.

3 Model

In this section, we present our jump-diffusion model and then describe the localized (event-based) specification of the model.

3.1 The General Form

Let X denote the N-dimensional vector, $X := [X_1, \ldots, X_N]'$, which represents the log-prices of N financial assets. We assume that the log-prices X follow an Itô semimartingale defined on a filtered space $(\Omega, \mathcal{F}_t, (\mathcal{F}_t)_{t\in[0,T]}, \mathbb{P})$ over a fixed time interval $[0, T]$. Under certain conditions (see Appendix A), we assume that the stock log-returns follow the dynamics given by

$$dX_{i,t} = b_{i,t}dt + \sigma_{i,t}dW_{i,t} + \xi_{i,t}dJ_{i,t}, \qquad i = 1, \ldots, N, \tag{1}$$

where $b_t := [b_{1,t}, \ldots, b_{N,t}]'$ is the vector of drifts, $W_t := [W_{1,t}, \ldots, W_{N,t}]'$ is the vector of Standard Brownian Motions and $J_t := [J_{1,t}, \ldots, J_{N,t}]'$ denotes an N-dimensional vector of jump processes of stocks with the vector of jump sizes denoted by $\xi_t := [\xi_{1,t}, \ldots, \xi_{N,t}]'$. We focus on the jump process J_t. To make the model match stylized features of *intradaily* jumps (see e.g., Boswijk et al., 2018; Dungey et al., 2018), we permit stochastic asset price jumps. That is,

$$d\lambda_{i,t} = \tilde{\alpha}_i(\lambda_{i,\infty} - \lambda_{i,t})dt + \tilde{\beta}_i dJ_{i,t}, \qquad i = 1, \ldots, N, \tag{2}$$

where $\lambda_{i,t} := [\lambda_{1,t}, \ldots, \lambda_{N,t}]'$ is the vector of stochastic jump intensity process (or scale) that captures the time-varying intensity of the extreme tail shocks. When the shocks $J_{i,t}$ hit the market (due to common news), trading activity typically surges and jump-type tail rallies of assets $\lambda_{i,t}$ increase with magnitude $\tilde{\beta}_i$. As the impact of the shock subsides, jump intensity reverts to its long-run mean $\lambda_{i,\infty}$, with speed

governed by $\tilde{\alpha}_i$.[5] The process (2) can incorporate high-frequency crashes, as emphasized in Aït-Sahalia et al. (2015) and motivated by Bates (2019) from an asset pricing perspective.

We next move from this general specification to an event-based specification by looking at the stochastic jump intensities, $\lambda_{i,t}$, of all assets in the panel around event times.

3.2 The Event-Based Form

We seek to characterize the market-wide (systemic) tail risk that occurs when multiple assets jump together in response to announcements. To this end, we extend the univariate approach of Erdemlioglu and Yang (2022) to a multivariate setup, and explore the *local* (news-induced) tail behavior of asset returns.[6]

Suppose that a single FOMC announcement arrives at a known time, denoted $E_{s=1}$.[7] The dynamics of jump intensities at event times can be written as

$$d\lambda_{i,t}^{event} = \tilde{\alpha}_i(\lambda_{i,\infty}^{event} - \lambda_{i,t}^{event})dt + \tilde{\beta}_i dJ_{i,t}, \qquad i = 1, \ldots, N, \tag{3}$$

where $\lambda_{i,t}^{event} := [\lambda_{1,t}^{event}, \ldots, \lambda_{N,t}^{event}]'$ denotes the N-dimensional vector of the stochastic jump intensities of the N assets around each FOMC event (denoted by superscript *event*).[8]

How does news change the tail probability? If the FOMC event creates a jump with magnitude ξ, the news-induced tail probability ratio is

$$\frac{\mathbb{P}(|(\lambda_{i,\infty}^{event} + \xi)\Delta_n J_i| \geq \alpha\Delta_n^{\varpi})}{\mathbb{P}(|\lambda_{i,\infty}^{event}\Delta_n J_i| \geq \alpha\Delta_n^{\varpi})} \approx \left(\frac{\lambda_{i,\infty}^{event} + \xi}{\lambda_{i,\infty}^{event}}\right)^{\beta_i} = (1 + \xi/\lambda_{i,\infty}^{event})^{\beta_i}, \qquad i = 1, \ldots, N, \tag{4}$$

where the Δ_n is incremental change between observations, $\alpha\Delta_n^{\varpi}$ is the threshold to retain only very large jumps (to be defined later), and $\beta_i := [\beta_1, \ldots, \beta_N]'$ is the vector of jump activity indices controlling the vibrancy of fluctuations, serving as a tail measure similar to the estimator of Hill (1975).[9] For a given value of λ^{event}, if the news generates a jump with large magnitude (e.g., $\xi = 12$), the tail probability ratio will be around 1.8. That is, the FOMC event that induces this large jump ($\xi = 12$) in each asset will

[5] Under the conditions, $\tilde{\alpha}_i > \tilde{\beta}_i > 0$ and $\lambda_{i,\infty} > 0$.

[6] Supplementary Appendix B presents several motivating examples along with a schematic representation of our model.

[7] Because the event time is known, the jump time is deterministic but the jump magnitudes and tail behavior are still stochastic and are unrestricted.

[8] From the FOMC's viewpoint, the objective for traders in this regard would be to examine the market-wide, possibly adverse, consequences of the announcement.

[9] See the related discussion in p. 2209 in Aït-Sahalia and Jacod (2009a).

increase the likelihood of extreme change (both left- and right-tails) by 80%, compared with the case of no jumps. Such a substantial change in the tail probability implies that cojumping assets pose systemic tail risk.

This approach has several advantages compared to specifications in prior research (e.g., Caporin et al., 2017; Boswijk et al., 2018; Dungey et al., 2018; Aït-Sahalia et al., 2015; Erdemlioglu and Yang, 2022). First, our framework extends the methodology of Erdemlioglu and Yang (2022) to a multi-asset setting and introduces a new test. Second, unlike the conventional jumps-news *matching analysis*, our event-based approach explicitly permits us to assess the news effect and quantify its risk at high frequency. Third, we can formally identify whether apparent jumps are actually jumps or spurious jumps caused by volatility spikes (Section 4). By conditioning on the news event, we can minimize false jump discoveries. Last but not least, event-based testing extends the mutual excitation models (see e.g., Boswijk et al., 2018; Dungey et al., 2018) by incorporating the impact of a common event into asset price dynamics.

Having outlined the modeling framework, we next introduce our testing and detection procedures.

4 Methodology

This section first outlines the estimators required for the test statistics. Then Section 4.2 details our testing framework and discusses how to detect non-spurious systemic cojumps at high frequency, conditional on the arrival times of information events.

4.1 Estimation and Test Statistics

We estimate the latent jump intensity before presenting the tests for systemic effects. Following the definitions in Erdemlioglu and Yang (2022), let us consider *pre-* and *post-event* estimators for the jump intensity, $\widehat{\lambda}^{event}$. For each stock ($i = 1, \ldots, N$), we can write

$$\widehat{\lambda}_i(k_n)^{\text{event}} \begin{cases} \widehat{\lambda}_i(k_n)^{\text{pre}} := \frac{\Delta_n^{\varpi\widehat{\beta}_i}}{k_n\Delta_n} \sum_{j=1}^{k_n} g\left(\frac{|\Delta_j^n X_i^{(\text{pre})}|}{\alpha\Delta_n^{\varpi}}\right) \frac{\alpha^{\widehat{\beta}}}{C_{\widehat{\beta}_i}(k_n)} & \Longrightarrow \text{ (pre-event window)} \\ \widehat{\lambda}_i(k_n)^{\text{post}} := \frac{\Delta_n^{\varpi\widehat{\beta}_i}}{k_n\Delta_n} \sum_{j=1}^{k_n} g\left(\frac{|\Delta_j^n X_i^{(\text{post})}|}{\alpha\Delta_n^{\varpi}}\right) \frac{\alpha^{\widehat{\beta}}}{C_{\widehat{\beta}_i}(k_n)} & \Longrightarrow \text{ (post-event window),} \end{cases}$$

where, based on an integer k_n and certain functional forms $g(\cdot)$, $\widehat{\beta}_i$ is the estimator for the jump activity index of stock i, $C_{\widehat{\beta}_i}$ (see Appendix A for details), $\widehat{\lambda}_i(k_n)^{\text{pre}}$ and $\widehat{\lambda}_i(k_n)^{\text{post}}$ are the intensity estimators before and after the information arrivals, respectively, in the estimation windows. Note that both $\widehat{\lambda}_i(k_n)^{\text{pre}}$ and $\widehat{\lambda}_i(k_n)^{\text{post}}$ contain the high-frequency return variations $|\Delta_j^n X_i^{(\text{pre})}|$ and $|\Delta_j^n X_i^{(\text{post})}|$ for the pre- and post-event windows, respectively. We seek to detect whether or not $\widehat{\lambda}_i(k_n)^{\text{pre}}$ changes when the news arrives.

Specifically, we test for systemic cojumps (SCOJ), given the arrival of events. For all news events, we introduce the null and alternative hypotheses, respectively, as follows.

$$H_0: \quad \omega \in \Omega_T^{\text{noSCOJ}} := \Omega_t^{\lambda^{\text{event}},0} = \{\omega : \lambda(\omega)_{i,t}^{\text{pre}} = \lambda(\omega)_{i,t}^{\text{post}}\}, \qquad i = 1, \ldots, N, \tag{5}$$

vs.

$$H_a: \quad \omega \in \Omega_T^{\text{SCOJ}} \quad := \Omega_t^{\lambda^{\text{event}}} \quad = \{\omega : \lambda(\omega)_{i,t}^{\text{pre}} \neq \lambda(\omega)_{i,t}^{\text{post}}\}, \qquad i = 1, \ldots, N,$$

where ω denotes a specific outcome, $\omega \in \Omega$, for which we need to evaluate whether the outcome belongs to the set of "no systemic cojumps" ($\omega \in \Omega_T^{\text{noSCOJ}}$) or is a systemic cojump, i.e., ($\omega \in \Omega_T^{\text{SCOJ}}$). Under the null hypothesis of no systemic cojumps (5), we define our test statistics as follows, conditional on the timing of FOMC events:

$$\mathcal{T}_{i,t}^{(\text{event})} = \sqrt{\frac{k_n \Delta_n}{\Delta_n^{\varpi \widehat{\beta}_i}}} \frac{\widehat{\lambda}_{i,t}^{\text{post}} - \widehat{\lambda}_{i,t}^{\text{pre}}}{\left(\sqrt{\alpha_i^{\beta} C_\beta(2)(\widehat{\lambda}_{i,t}^{\text{post}} + \widehat{\lambda}_{i,t}^{\text{pre}})}\right) \Big/ C_\beta(1)}, \qquad i = 1, \ldots, N, \tag{6}$$

which traces how sharply λ changes after each news event.[10]

4.2 Detection Procedures and Theoretical Properties

The estimation of repeated jump tests creates the potential for multiple testing bias and false discovery, that is, erroneously rejecting the true null hypothesis of no jump.[11] We seek to minimize such bias.

[10] This statistic is asymptotically independent from that for volatility spikes. The conclusion still holds if we replace the deterministic time t with any $\mathcal{F}_t$-stopping time. To compute the test statistic in (6), we use the pre- and post-event estimators, $\widehat{\lambda}_{i,t}^{\text{post}}$, $\widehat{\lambda}_{i,t}^{\text{pre}}$, the asset-specific jump activity index, $\widehat{\beta}_i$ along with certain parameters, including k_n, Δ, α and C_β. These technical insights and implementation details are unreported for brevity yet they are available upon request.

[11] Bajgrowicz et al. (2016) and Romano and Wolf (2005) discuss multiple testing bias in depth.

Statistically, we cope with the data snooping problem in three ways: First, we account for the dependence structure of test statistics given by (6). Second, we asymptotically control for the family-wise error rate (FWE) at a given nominal level. Third, to maximize detection power, that is, to reject *as many false* null hypotheses as possible, we extend the stepwise method of Romano and Wolf (2005) to condition on events.[12] We have the following result:

Theorem 1 (Bootstrap Consistency)**.** *Suppose that Assumptions 1, 2 and 3 hold (See Appendix). Then the following statements concerning Algorithm 1 are true.*

(i) When the null hypothesis is false, the event-based StepM algorithm will reject the null hypothesis with probability 1 as $n \to \infty$.

(ii) The event-based StepM algorithm asymptotically controls the familywise error rate (FWE) at level α*; that is,* $\lim_n FWE_{\mathbb{P}} \leq \alpha$.

This result ensures that the bootstrap consistently estimates the limiting distribution of our test statistic (see Appendix A and C for the proof and algorithm, respectively).[13] Further, we provide the bootstrap Central Limit Theorem (CLT) for the jump intensity estimator as follows.

Theorem 2 (Bootstrap CLT for Jump Intensity Estimator)**.** *Under Assumptions 1–3 and the following conditions:*

1. *Scaling:* $k_n^\lambda \Delta_n^{1-\varpi\beta} \to 0$ *as* $\Delta_n \to 0$,
2. *Truncation function:* $g_n(x) = g(x/\alpha\Delta_n^\omega)$*, where* $g(\cdot)$ *satisfies Assumption 3,*
3. *Jump activity:* $\beta \in (0,2)$*, and* $\varpi \in (0,1/2)$,

the bootstrap estimator satisfies:

$$\sqrt{\frac{k_n^\lambda \Delta_n}{\Delta_n^{\varpi\beta}}}\left(\widehat{\lambda}(\widehat{\beta}, k_n^\lambda)_t^* - \widehat{\lambda}(\widehat{\beta}, k_n^\lambda)_t\right) \xrightarrow{L^*} N\left(0, \lambda_{t+}\frac{\alpha^{2\beta}C_\beta(2)}{[C_\beta(1)]^2}\right),$$

[12] Our definition of *power* follows the notion of average power considered in Romano and Wolf (2005), which refers to the expected number of false hypotheses rejected. See Supplementary Appendix C for the implementation details.

[13] It is worth mentioning that, unlike Romano and Wolf (2005), we implement the StepM procedure to each event timing rather than considering averages (i.e., average historical returns). See Examples 2.1 and 2.2 (pp. 1240 and 1241) in Romano and Wolf (2005), respectively. Nevertheless, our approach is still computationally tractable, although we implement the full system via bootstrap. For instance, while Romano and Wolf (2005) use 105 test statistics, we consider 2332 test statistics in our empirical analysis.

where $\xrightarrow{L^*}$ *denotes convergence in law under the bootstrap measure* $\mathbb{P}^*$.

We can further generalize Theorem 2 to explicitly allow for cross-sectionally dependent jumps, e.g., when systemic cojumps driven by common events. Theorem 3 extends Theorem 2 and gives the Bootstrap CLT for dependent systemic jumps.

Theorem 3 (Bootstrap CLT for Dependent Systemic Jumps)**.** *We have the following additional assumptions.*

(A4) Dependent Jump Measure: The jump measure decomposes as $\mu = \mu^{\text{idiosyncratic}} + \mu^{\text{systemic}}$*, where* μ^{systemic} *captures simultaneous cojumps across assets driven by systemic events (e.g., FOMC announcements).*

(A5) Orthogonality: $\mu^{\text{idiosyncratic}} \perp \mu^{\text{systemic}}$ *(mutually orthogonal jump measures).*

(A6) Block Dependence: Systemic jumps exhibit weak temporal dependence, i.e., $\alpha(m) = O(m^{-a})$ *for* $a > 1$*, where* $\alpha(m)$ *is the mixing coefficient over* m*-separated blocks.*

Under Assumptions 1–3 and (A4)–(A6), and the scaling $k_n^\lambda \Delta_n^{1-\varpi\beta} \to 0$*,*

$$\sqrt{\frac{k_n^\lambda \Delta_n}{\Delta_n^{\varpi\beta}}} \left(\widehat{\lambda}(\widehat{\beta}, k_n^\lambda)_t^* - \widehat{\lambda}(\widehat{\beta}, k_n^\lambda)_t \right) \xrightarrow{L^*} N\left(0, \lambda_t^{\text{idiosyncratic}} \frac{\alpha^{2\beta} C_\beta(2)}{[C_\beta(1)]^2} + \lambda_t^{\text{systemic}} \frac{\alpha^{2\beta} C_\beta(2)}{[C_\beta(1)]^2}\right),$$

where $\xrightarrow{L^*}$ *denotes convergence in law under the bootstrap measure* $\mathbb{P}^*$.

Another challenge is that large and sharp changes in prices $|\Delta_j^n X_i^{(\text{post})}|$ may not really be jumps, either because they might result from jumps in volatility or because they might be falsely identified large diffusion returns. We deal with this challenge by controlling for volatility jumps. Theorem 4 ensures that volatility jumps do not distort the detection of systemic cojumps in stochastic intensity.

Theorem 4 (Bootstrap Validity Under Volatility Jumps)**.** *Consider the DGP (D.8)–(D.10) (see Appendix D) with stochastic volatility jumps (i.e.,* $\theta \neq 0$ *in (D.9)). Under the following assumptions:*

(i) The volatility jump size satisfies $\theta = O(\Delta_n^{1/2})$.

(ii) The block length ℓ_n *for bootstrap resampling satisfies* $\ell_n = o(\Delta_n^{-1/2})$.

(iii) The truncation function $g_n(x)$ in (4) satisfies Assumption 3 (bounded, smooth, and truncates increments below $\alpha\Delta_n^\omega$).

the bootstrap critical values $\hat{c}_j$ computed via Algorithm 2 remain consistent for the max statistic $\max_{1\le i\le N}\mathcal{T}_{i,t}^{(\text{event})}$. Consequently, the StepM method asymptotically detects jumps exclusively in the stochastic jump intensity $\lambda_{i,t}$, even when volatility jumps occur:

$$\sup_{x\in\mathbb{R}}\left|\mathbb{P}^*\left(\max_{1\le i\le N}\mathcal{T}_{i,t}^{(\text{event}),*}\le x\right)-\mathbb{P}\left(\max_{1\le i\le N}\mathcal{T}_{i,t}^{(\text{event})}\le x\right)\right|\xrightarrow{\mathbb{P}}0.$$

Before conducting our empirical analysis, we evaluate the properties of our detection approach via Monte Carlo simulations. As Section 5 details our Monte Carlo study, the results reveal that the test statistics have good power after the bias correction, suggesting that our StepM bootstrap method effectively mitigates false discoveries, unlike the uncorrected test. We provide Theorem 5 which formalizes this result.

Theorem 5 (False Discovery Control via StepM Bootstrap)**.** *We have the following assumptions.*

(A7) Multiple Testing Framework: For N assets, the null hypothesis $H_{0,i}:\lambda_{i,t}=0$ (no cojump in asset i at time t) is tested using the statistic $T_{i,t}=\sqrt{\frac{k_n^\lambda\Delta_n}{\Delta_n^{\varpi\beta}}}\left(\widehat{\lambda}_{i,t}-\lambda_{i,t}\right)$.

(A8) Weak Cross-Sectional Dependence: The test statistics $\{T_{i,t}\}_{i=1}^N$ are weakly dependent across assets, satisfying an α-mixing condition with $\alpha(m)=O(m^{-a})$ for $a>1$.

(A9) Bootstrap Validity for Maxima: The bootstrap consistently approximates the distribution of the maximum statistic:

$$\sup_{x\in\mathbb{R}}\left|\mathbb{P}^*\left(\max_{1\le i\le N}T_{i,t}^*\le x\right)-\mathbb{P}\left(\max_{1\le i\le N}T_{i,t}\le x\right)\right|\xrightarrow{\mathbb{P}}0.$$

- If critical values are calibrated without StepM (e.g., using the marginal $N(0,1)$ distribution), the probability of at least one false discovery (FWER) satisfies:

$$\lim_{N\to\infty}\mathbb{P}\left(\textit{Reject } H_{0,i} \textit{ for some } i\mid H_0\right)=1.$$

- *Under (A7)–(A9), the StepM-adjusted critical value $\widehat{c}^{*}_{1-\alpha}$ controls FWER asymptotically:*

$$\limsup_{N\to\infty} \mathbb{P}\left(\textit{Reject } H_{0,i} \textit{ for some } i \mid H_0\right) \leq \alpha.$$

We now turn to examining the properties of our proposed test on simulated data.

5 Monte Carlo Study

Data generating process (DGP): We simulate an N-dimensional jump-diffusion process where the stochastic intensity process is allowed to jump with the arrival of the news events. In line with our discussion in the main text (see Section 3.2), we allow the stochastic volatility process to exhibit jumps. For each stock ($i = 1, \ldots, N$), the underlying DGP for log-returns is as follows.

$$dX_{i,t} = \sigma_{i,t} dW_{i,t} + \lambda_{\infty} dJ_{i,t} \tag{7}$$

$$d\sigma^2_{i,t} = \kappa(\theta - \sigma^2_{i,t}) + \eta\sigma_{i,t}(\phi dW_{i,t} + \sqrt{(1-\phi^2)} dB_{i,t}) + \theta 1_{\{S=JT\}} \tag{8}$$

$$d\lambda_{i,t} = \kappa_{\lambda}(\lambda_{i,\infty} - \lambda_{i,t})dt + \eta_{\lambda} dB'_{i,t} + \xi\, 1_{\{S=JT\}}, \tag{9}$$

where S and JT denote event time and jump time, respectively, and the vector of Brownian motion ($W_{i,t}$, $B_{i,t}$, $B'_{i,t}$) and the vector of β-stable jump processes $J_{i,t}$ are independent from each other. In (9), we use λ_{∞} to capture a tail probability of 0.25% (see our discussion in the main text in Section 3.2). We choose $\alpha = 5$ to separate the diffusion component from the jumps (see Equation (4) in the main text).

Selection of parameters and thresholds. We follow Jing et al. (2012) and choose the parameter values as follows: $\kappa = 5$, $\theta = 1/16$, $\eta = 0.5$, $\phi = -0.5$ (i.e., the leverage effect between between prices and volatility), $\eta_{\lambda} = 50$ and $\kappa_{\lambda} = 80$ which controls for the persistence of jumps or speed of decay (i.e., mean-reversion) of jump-type tail shocks. Increasing κ_{λ} implies lower persistence or higher speed of decay. Further, we consider a set of β (jump activity index) values. In all simulations, $T = 1/252$, $\varpi = 1/3$, $\rho = 0.6$, as in Aït-Sahalia and Jacod (2009a), Jing et al. (2012) and Dungey et al. (2018). We use 6.5 hours of trading during the day. We evaluate the performance of the tests based on 15-seconds and 1-minute sampling frequencies (i.e., which corresponds to number of intraday observations per day $M = 1560$, $M = 390$, respectively).

Implementation. Given the selected parameters and calibration values, we generate data based on the dynamics given in (7)−(9). For each replication, we simulate testing time points (representing event times S) that are same for all N assets. We then allow each asset to jump at these pre-determined time points, that is, when jump times (JT) coincide with event times (see the indicator function for $S = JT$ in (9)). After determining the pre- and post-event window, (by realistically setting as within hour before and after the event times), we compute the estimators (see Section 4.1). The final stage of the implementation of our Monte Carlo study is to apply the procedures presented in Algorithms 1 and 2 (see Sections 4.2 and Appendix C, respectively).

Simulation results and discussion. Table S.1 reports the frequency of rejections in the presence of systemic cojumps conditional on news arrival times (i.e., when $S = JT$). The simulation case that is consistent with our empirical setup is reported in Panel B (i.e, $N = 20$ and $S = 10$ at the yearly basis). The results indicate that the base test (labeled as "uncorr") has a detection rate which is around 97% at the 5% level. Once we control for multiple test bias via StepM, however, the power is relatively stable at 1-min frequency while it declines to 87% at 15-seconds frequency. It is worth mentioning that 87% rejection rate does not directly indicate low detection power (or poor performance), compared to base test. Rather, the StepM rejection rates account for false discovery and hence provide power that is more conservative (implying lower probability of rejecting false hypotheses). Thus, StepM rates are more reliable. The results also show that StepM has a higher power than one-step-only correction (labeled as "Step-1" in the panel). Nevertheless, when we consider only one event ($S = 1$ instead of $S = 10$), the power of StepM increases in simulations.

In addition these results, Panel A of Table S.1 reports the rejection rates when $N = 200$. The tests overall generate quite reasonable power, although the power of StepM based on 1-min sampling has a power around 73%. As a final assessment, we rely on the simulation setup reported in Panel B, but lower the jump size by about half. In other words, we consider a situation in which news arrives but creates a small jump. As the rejection rates in Panel C reveal, we observe significant power loss in all tests, irrespective of S or sampling frequency (1 min or 15-seconds). This pattern suggests that our tests require a very large jump to generate reasonable detection power (Panel B versus Panel C). If the jump size is small in response to news, perhaps not surprisingly, the tests are not able to identify systemic cojumps, as tests fail to disentangle jumps from extreme volatility.

We proceed by introducing the data and then discussing our results, respectively.

6 Data

This section describes our high-frequency data and news announcements.

6.1 Stock Market Data

Our data consist of high-frequency data on twenty-two individual stocks listed in Dow Jones Industrial Average (DJIA) and nine SPDR sector ETFs. We create equally-spaced observations at 15-second sampling frequency using raw (tick-by-tick) data from the WRDS. We assess the systemic effects of news events on sector ETF portfolios, as investors often use them for tactical asset allocation and sector-rotation strategies. The first three columns of Table 1 list the tickers, names, and industries of the stocks and sector ETFs. The sample spans January 31, 2006 through January 30, 2019.

We adjust the data in the usual ways. We discard the sample days with excessively low trading activity, missing price observations, empty (zero data) intervals and consecutive (unchanged) transaction prices. As is standard, we exclude U.S. holidays (fixed/irregular), Christmas periods and weekends from our sample. For both individual stocks and sector ETFs, we only use trading hours (9:30 EST−16:00 EST), not overnight observations. To minimize market microstructure noise, we filter out the *bouncebacks* associated with bid-ask spreads and irregular quotes. This reduces spurious price spikes and the impact of noise.

6.2 FOMC Announcements and Monetary Policy Shocks

Our event set includes scheduled announcements, which contain FOMC statements and interest rate decisions. We crosscheck published event times with Bloomberg and media articles. Our sample contains 106 FOMC announcements from January 31, 2006 through January 30, 2019.

Table 1 reports three types of summary statistics for Dow Jones stocks (Panel I) and sector ETFs (Panel II) from windows before and after FOMC news releases. FOMC events significantly change both stock and ETF returns (post-X versus pre-X) and realized volatility (post-RV versus pre-RV).[14] Announcements also

[14] In line with this pattern, realized volatility of all sector portfolios increases rapidly as soon as the news is released, see Figure S.1 in Supplementary Appendix.

Table 1: Descriptive statistics before and after the exact times of the FOMC announcements

Ticker	Company name	Industry	Pre-X	Post-X	ΔX	Pre-RV	Post-RV	RV ratio	Pre-SK	Post-SK
Panel I. Dow Jones stocks										
AAPL	Apple	Tech	0.025	0.026	0.000	0.119	0.239	2.014	0.826	-0.644
AXP	American Express	Fin. Services	0.054	0.171	0.118	0.123	0.284	2.314	1.260	1.124
BA	Boeing	Aerospace	-0.098	0.035	0.134	0.124	0.254	2.042	0.536	-0.045
CAT	Caterpillar	Construction	0.017	0.060	0.043	0.124	0.284	2.299	-1.562	0.582
CSCO	Cisco Systems	Tech	-0.066	0.059	0.125	0.145	0.255	1.761	0.217	0.194
CVX	Chevron	Oil & Gas	-0.017	0.044	0.061	0.111	0.239	2.155	-0.478	0.761
DIS	Disney	Entertainment	0.046	0.049	0.003	0.114	0.246	2.150	1.554	0.047
HD	Home Depot	Retail	0.047	0.206	0.159	0.114	0.253	2.223	1.654	0.846
IBM	IBM	Tech	0.026	0.063	0.038	0.093	0.207	2.231	-0.185	0.179
INTC	Intel	Tech	0.050	0.138	0.088	0.146	0.259	1.770	-0.557	-0.155
JNJ	Johnson & Johnson	Pharmaceuticals	0.010	0.071	0.062	0.080	0.171	2.123	-1.802	-0.504
KO	Coca-Cola	Food and Bev.	0.001	0.129	0.129	0.090	0.187	2.071	-0.469	-0.330
MCD	McDonald's	Food	0.032	0.016	-0.015	0.085	0.182	2.145	1.157	0.307
MMM	3M	Conglomerate	0.020	0.115	0.095	0.095	0.231	2.435	-0.630	0.310
MRK	Merck	Pharmaceuticals	0.002	0.331	0.329	0.114	0.229	2.004	-0.623	1.020
MSFT	MSFT	Tech	0.024	0.027	0.003	0.125	0.238	1.899	-0.440	0.493
NKE	Nike	Apparel	-0.032	0.183	0.215	0.110	0.241	2.200	-0.016	0.369
PFE	Pfizer	Pharmaceuticals	-0.005	0.085	0.090	0.138	0.232	1.681	0.883	0.695
UNH	UnitedHealth	Health Care	0.020	0.141	0.122	0.122	0.277	2.265	0.159	-0.185
VZ	Verizon	Telecom	0.033	-0.018	-0.052	0.107	0.215	2.008	1.412	-0.244
WMT	Wal-Mart	Retail	0.009	-0.064	-0.073	0.088	0.182	2.055	2.283	-0.183
XOM	Exxon Mobil	Oil & Gas	-0.033	0.048	0.081	0.102	0.221	2.166	-1.056	0.901
Panel II. Sector ETFs										
XLB	.	Materials	0.009	0.138	0.130	0.095	0.247	2.604	-0.156	0.168
XLE	.	Energy	-0.040	0.150	0.190	0.107	0.258	2.415	-1.825	0.863
XLF	.	Financials	0.005	0.111	0.106	0.143	0.294	2.062	-2.323	0.236
XLI	.	Industrials	0.004	0.120	0.116	0.085	0.222	2.619	-0.728	0.809
XLK	.	Technology	0.001	0.133	0.133	0.094	0.222	2.353	-0.924	0.323
XLP	.	Consumer Staples	-0.004	0.066	0.070	0.078	0.181	2.313	-1.018	0.583
XLU	.	Utilities	0.001	0.137	0.136	0.095	0.232	2.433	0.225	0.636
XLV	.	Health Care	-0.006	0.109	0.114	0.077	0.189	2.456	-0.833	0.657
XLY	.	Consumer Disc.	-0.005	0.079	0.083	0.084	0.227	2.717	-1.583	0.550

Notes: The table reports the descriptive statistics of high-frequency returns, realized volatility and skewness before and after the exact (intraday) times of FOMC news announcements. The table presents the values for twenty-two individual Dow Jones stocks (Panel I) and nine sector ETFs (Panel II). The sample covers the periods from January 31, 2006 to January 30, 2019, and contains 106 FOMC policy announcements. For each Dow Jones stock and sector ETF, the summary statistics reported in table are the averages across events. The first three columns, respectively, provide the tickers, company name and industry classifications. ΔX is the difference between post- and pre-FOMC returns, and RV ratio is the ratio of post-FOMC realized volatility to pre-FOMC realized volatility.

consistently and substantially change ETF realized skewness (see post-SK versus pre-SK). Taken together, these empirical features appear to corroborate the view that news often prompts traders to reevaluate their expectations and investment strategies.

To measure the news surprise associated with each FOMC event, we estimate the target factor and path factors, as in Gürkaynak et al. (2005), and the zero-bound factor, as in Wright (2012) (henceforth the Wright surprise).[15] We also construct a fed funds target change indicator to examine the systemic

[15]The target surprise is essentially the surprise change in overnight interest rates. The path surprise is orthogonal to the target surprise and empirically seems to be similar to the change in the 12-to-15-month forward rate. The Wright surprise is constructed from the change in the first principal component of high-frequency yield curve movements at announcement

Figure 1: Estimated U.S. monetary policy shocks

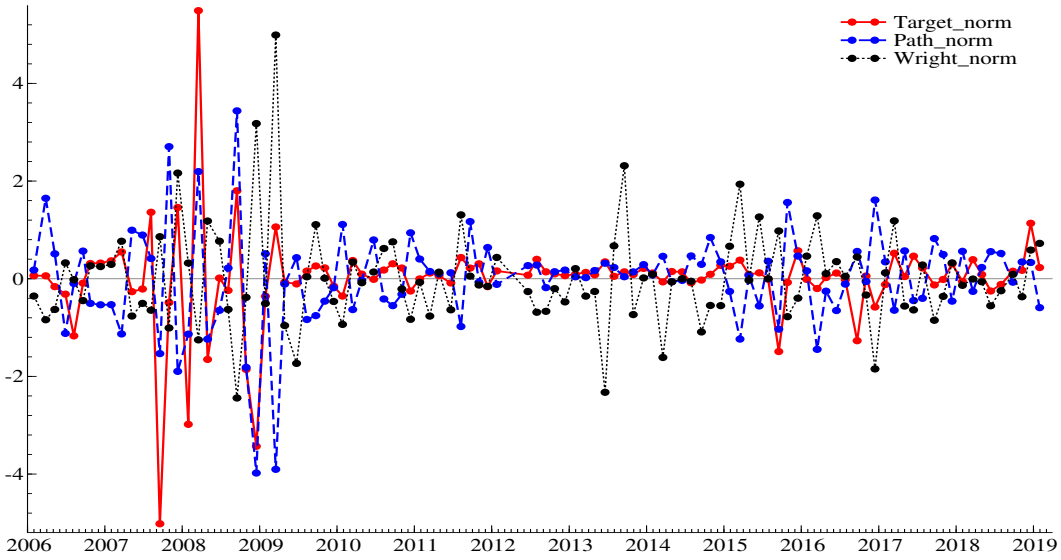

Notes: The figure shows the evolution of the estimated U.S. monetary policy shocks over time. We estimate the target and path shocks following the studies of Gürkaynak et al. (2005) and Wright (2012). In addition to these two (common) shocks factors, we construct the third surprise factor as the change in the level of yield curve (labeled as "Wright" in the figure). The sample contains 106 FOMC policy announcements from January 31, 2006 to January 30, 2019. All shock factors are normalized. The Y-axis denotes the value of the shock and X-axis denotes the periods (i.e., corresponding to news release times of FOMC meetings) in our sample. Supplementary Appendix D outlines the construction of monetary policy shocks. The methodological documentation is available upon request.

risk effects of conventional announcements. We call this variable a revision factor.

Figure 1 displays the estimated values of these three shocks over time. The shocks were large during the Great Financial Crisis of 2007-2009 and during the Fed's liftoff from the zero lower bound (ZLB) in 2015-2017. Each surprise factor captures distinct empirical features, as the signs and sizes of shocks appear to be different over time in periods of policy announcements.

7 Results

We start our assessment of the systemic risk effects of FOMC announcements by examining the summary statistics pertaining to news-driven systemic cojumps. Section 7.2 then links monetary policy shocks to systemic jump-response of stocks to FOMC news. Section 7.3 characterizes the most systemically

times. Appendix D describes the construction of these three types of monetary policy surprises. The implementation codes are available upon request.

important FOMC events, and Section 7.4 focuses on the role of QE announcements in downside risk. We construct Fed-driven systemic risk indicators in Section 7.5 and study two aspects of systemic tail risk. First, we examine the link between systemic tail risk and pre-FOMC announcement drift. Second, we explore whether Fed-driven systemic tail risk increases variance risk premia (Sections 7.6 and 7.7, respectively).

7.1 Presence of News-Driven Systemic Cojumps and Crashes

We begin by identifying systemic cojumps, conditional on the times of the FOMC announcements. We compute the cojump test statistic (given in Equation (6)) on the prices of the 22 individual stocks and 9 sector ETFs for each of the 106 FOMC announcements. We then apply the conditional StepM algorithm (Section 4.2) to reduce spurious detection. While we use all returns for detecting systemic cojumps, we take only negative returns in assessing whether FOMC news results in crashes and downside tail risk.

Table 2: Summary statistics for the FOMC-driven systemic cojumps and crashes

	Events	Assets	Mean	Frac	Stdev	Max	Min	Thr
Panel I. Dow Jones stocks								
SCOJ	106	22	12.77	0.58	7.76	22	0	0.48
SCRA	106	22	5.75	0.26	7.61	22	0	0.20
Panel II. Sector ETFs								
SCOJ	106	9	4.93	0.55	3.51	9	0	0.50
SCRA	106	9	2.08	0.23	2.91	9	0	0.18

Notes: The table reports the summary statistics for the detected systemic cojumps (SCOJ) and crashes (SCRA), conditional on the times of the FOMC announcements. The table shows the number of events used in the testing procedures ("Events"), the number of assets ("Assets"), the average number of systemic cojumps for each announcement in the sample ("Mean"), the fraction of assets that cojump together out of all assets (i.e., "Frac" (= Mean/Assets)), standard deviation of the number of systemic cojumps ("Stdev") and max-min values ("Max", "Min"). The last column ("thr") gives the threshold-based average, which is the fraction of periods in which at least two-thirds of the assets cojump together. The sample covers January 31, 2006 to January 30, 2019. The sampling frequency is 15-seconds.

Table 2 reports the summary statistics for the detected systemic cojumps and crashes. Panel I shows that systemic cojumps arrive very frequently. For instance, an average of 12.77 (or 58%) of Dow Jones stocks cojump simultaneously in response to FOMC news (columns 4 and 5). Nearly half of all FOMC events (0.48) cause at least two-third of the Dow Jones stocks to jump simultaneously (last column). Panel II of the table shows that sector ETFs cojump much like individual stocks, suggesting that such funds

cannot diversify systemic jump risk.

The "SCRA" rows in Table 2 show that FOMC news often produces crashes, i.e., downward systemic cojumps. On average, 5.75 Dow Jones stocks (out of 22) and 2.08 ETFs (out of 9) crash together in response to FOMC events. The high number of stocks crashing together is likely to impair hedging cojumps from an FOMC decision, particularly if the news leads to such crashes.

7.2 FOMC Announcements, Monetary Policy and Systemic Reaction

We now ask the following questions: How do the frequency and size of FOMC-driven systemic cojumps/crashes evolve over time? What is the role of the surprise in triggering systemic jumps?

The middle and lower panels of Figure 2 illustrate the respective number of DJ stocks and sector ETFs that take part in FOMC-driven cojumps and crashes. The cojump/crash statistics for stocks and ETFs follow similar time-varying patterns. Larger monetary policy surprises induce more systemic jumps and these occur mostly during 2008-2009, during which FOMC news commonly produces downward cojumps. Systemic effects become rarer after 2010, with no identified crashes during 2012 and early 2013 (dashed red lines), a period with no significant downside monetary surprises.[16] Systemic cojump risk rebounded in 2014-2015 before again giving way to relative calm in 2016-2017. The news surprise (upper panel) tends to explain the strength of identified systemic reaction.

7.3 Systemically Important News Events

The evidence in the previous section suggests that diversifying cojump risk is likely to be more challenging than previously thought because ETF jump characteristics are similar to those of individual stocks. With an event-induced cojump/crash detection approach, we can rank which FOMC events create the most widespread systemic risk.[17]

We compile the list of systemically important news events (SINE) as follows: First, we detect systemic cojumps (SCOJ) and crashes (SCRA) in the data, conditional on the FOMC announcements. Then, we compute the fraction of assets that jump (and crash) together among all assets and rank the events by the fractions of jumping assets based on SCOJ and SCRA, respectively.

[16] The "Taper Tantrum" of May-June 2013 was a significant contractionary surprise.

[17] It is worth reemphasizing that our definition of systemic risk directly follows those of Caporin et al. (2017) and Das and Uppal (2005). High-frequency (intradaily) systemic risk occurs when more-than-two assets cojump, irrespective of the signs or magnitudes. That is, the crashes are downward cojumps in asset prices.

Figure 2: Monetary policy shocks, systemic cojumps and crashes

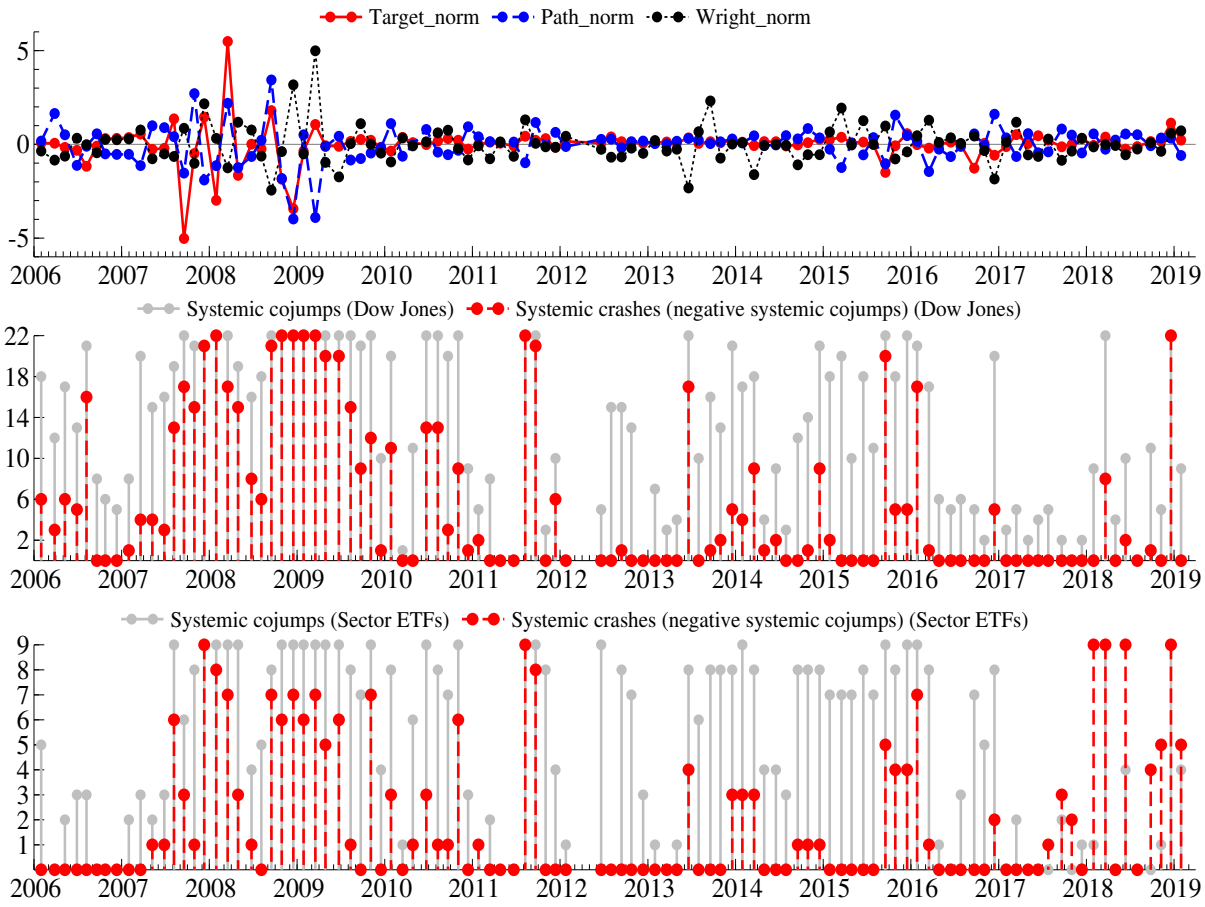

Notes: The upper panel of the figure displays the time series of estimated monetary policy shocks while the middle and lower panels show the number of detected systemic cojumps and crashes for DJ stocks and sector ETFs, respectively. Figure 1 describes the target/path/wright factors. In the middle and lower panels, the solid (dashed) gray (red) lines with filled circles indicate the number of systemic cojumps (crashes), respectively. Crashes are downward systemic cojumps. The sample covers January 31, 2006 to January 30, 2019, and contains 106 FOMC policy announcements.

Tables 3 and 4 report our SINE ranking (top 20), based on the panels of individual stocks and sector ETF portfolios, respectively. Every FOMC event in Table 3 produces jumps in every stock and many of them produce systemic crashes. That is, frac(SCOJ) equals one for all these events and frac(SCRA) equals one for seven of these events.

In other words, these events spur all 22 individual stocks to jump at the same time and induce crashes. Most of the systemically important FOMC events take place during the Great Financial Crisis and its aftermath, from 2008-2010 (fifteen events). Announcements since 2011 have fewer systemic consequences. Only three of the top 20 events occurred after January 1, 2012: the FOMC decisions released on December

Table 3: Systemically important news events based on cojumps and crashes of Dow Jones stocks

Date	Rank	SCOJ	frac(SCOJ)	SCRA	frac(SCRA)	Target	Path	Wright
2008-01-30	1	22	1.00	22	1.00	-2.983	-1.134	0.321
2008-10-29	2	22	1.00	22	1.00	-1.859	-1.816	-0.383
2008-12-16	3	22	1.00	22	1.00	-3.433	-3.979	3.178
2009-01-28	4	22	1.00	22	1.00	-0.359	0.511	-0.508
2009-03-18	5	22	1.00	22	1.00	1.060	-3.904	4.991
2011-08-09	6	22	1.00	22	1.00	0.433	-0.978	1.307
2018-12-19	7	22	1.00	22	1.00	1.135	0.333	0.587
2008-09-16	8	22	1.00	21	0.95	1.802	3.438	-2.443
2011-09-21	9	22	1.00	21	0.95	0.218	1.170	0.053
2009-04-29	10	22	1.00	20	0.91	-0.072	-0.109	-0.959
2009-06-24	11	22	1.00	20	0.91	-0.106	0.431	-1.735
2015-09-17	12	22	1.00	20	0.91	-1.492	-1.033	0.979
2007-09-18	13	22	1.00	17	0.77	-5.019	-1.533	0.861
2008-03-18	14	22	1.00	17	0.77	5.490	2.195	-1.252
2013-06-19	15	22	1.00	17	0.77	0.345	0.317	-2.326
2009-08-12	16	22	1.00	15	0.68	0.157	-0.835	0.039
2010-06-23	17	22	1.00	13	0.59	-0.012	0.794	0.138
2010-08-10	18	22	1.00	13	0.59	0.179	-0.415	0.619
2009-11-04	19	22	1.00	12	0.55	0.222	-0.460	0.010
2010-11-03	20	22	1.00	9	0.41	0.219	-0.318	-0.211

Notes: The table ranks 20 FOMC events from systemically most to least important in terms of creating systemic cojumps and crashes. The table reports the date of the event (first column), the rank (second column), the number of assets that cojump and crash (downward cojump) together after each event ("SCOJ" and "SCRA"). The results are based on tests applied to 22 individual stocks. The table further presents the fraction of assets that cojump or crash together out of all 22 assets (i.e., frac(SCOJ) = SCOJ/22, frac(SCRA) = SCRA/22). To construct the ranking, we sort the fractions by SCOJ and then by SCRA. In the last three columns, we provide the normalized estimates of target, path and Wright factors (at announcements times) capturing monetary policy shocks (see Figure 1 for details). Negative (positive) values for Wright shocks represent contractionary (expansionary) shocks. The sample covers January 31, 2006 to January 30, 2019.

19, 2018, September 17, 2015, and June 19, 2013 (see Table 3).[18]

7.4 Systemic Effects of Unconventional Monetary Policy Announcements

Having identified the key systemic FOMC events, we now evaluate whether or not unconventional monetary policy (UMP) news spark systemic effects.[19] Fratzscher et al. (2018) is the source of our list of UMP events,

[18]The December 19, 2018 statement was not as dovish as markets expected. The FOMC unexpectedly declined to raise rates at its September 17, 2015 meeting, which would have been its first federal funds rate increase since the Great Financial Crisis. Finally, June 19, 2013 was the date of the "taper tantrum".

[19]Practitioners and researchers have long sought to understand the financial and economic impact of UMP policies, see e.g., Di Maggio et al. (2020); Hayashi and Koeda (2019); Fratzscher et al. (2018); Rodnyansky and Darmouni (2017); Kapetanios et al. (2012); Christensen and Rudebusch (2012) and Joyce et al. (2012).

Table 4: Systemically important news events based on cojumps and crashes of sector ETFs

Date	Rank	SCOJ	frac(SCOJ)	SCRA	frac(SCRA)	Target	Path	Wright
2007-12-11	1	9	1.00	9	1.00	1.459	-1.898	2.164
2011-08-09	2	9	1.00	9	1.00	0.433	-0.978	1.307
2018-03-21	3	9	1.00	9	1.00	0.391	-0.259	-0.006
2018-12-19	4	9	1.00	9	1.00	1.135	0.333	0.587
2008-01-30	5	9	1.00	8	0.89	-2.983	-1.134	0.321
2011-09-21	6	9	1.00	8	0.89	0.218	1.170	0.053
2008-03-18	7	9	1.00	7	0.78	5.490	2.195	-1.252
2008-12-16	8	9	1.00	7	0.78	-3.433	-3.979	3.178
2009-03-18	9	9	1.00	7	0.78	1.060	-3.904	4.991
2009-11-04	10	9	1.00	7	0.78	0.222	-0.460	0.010
2016-01-27	11	9	1.00	7	0.78	-0.013	0.163	0.462
2007-08-07	12	9	1.00	6	0.67	1.361	0.414	-0.646
2008-10-29	13	9	1.00	6	0.67	-1.859	-1.816	-0.383
2009-01-28	14	9	1.00	6	0.67	-0.359	0.511	-0.508
2009-06-24	15	9	1.00	6	0.67	-0.106	0.431	-1.735
2010-11-03	16	9	1.00	6	0.67	0.219	-0.318	-0.211
2009-04-29	17	9	1.00	5	0.56	-0.072	-0.109	-0.959
2015-09-17	18	9	1.00	5	0.56	-1.492	-1.033	0.979
2015-12-16	19	9	1.00	4	0.44	0.574	0.465	-0.399
2008-04-30	20	9	1.00	3	0.33	-1.652	-1.239	1.182

Notes: The table ranks 20 FOMC news from systemically most to least important in terms of creating systemic cojumps and crashes. The table reports the date of the event (first column), the rank (second column), the number of assets that cojump and crash (downward cojump) together after each event ("SCOJ" and "SCRA"). The results are based on tests applied to 9 sector ETFs. The table further presents the fraction of assets that cojump or crash together out of all 9 assets (i.e., frac(SCOJ) = SCOJ/9, frac(SCRA) = SCRA/9). To construct the ranking, we sort the fractions by SCOJ and then by SCRA. In the last three columns, we provide the normalized estimates of target, path and Wright factors (at announcements times) capturing monetary policy shocks (see Figure 1 for details). Negative (positive) values for Wright shocks represent contractionary (expansionary) shocks. The sample covers the periods from January 31, 2006 to January 30, 2019.

which are related to the Fed's QE1 and QE2 programs.[20] Table 5 reports the test results for QE1 and QE2 events.

Two UMP announcements produced very large crash statistics: the FOMC statements on December 16, 2008 (third row) and March 18, 2009 (fifth row). The December 16 announcement included a federal funds target cut, a suggestion that the Fed might purchase Treasuries and forward guidance that the FOMC expects low rates "for some time". The March 18, 2009 statement announced very large Fed purchases of $300 billion in long-term Treasuries and $750 and $100 billion in MBS and GSE debt, respectively. In addition, the FOMC strengthened its forward guidance to expect low rates "for an extended period" (column 4 in the table). There is very strong evidence for systemic cojumps after these events; the average SCOJ statistics for these two news releases are 11.80 and 11.05, respectively, the largest among all listed

[20]The results with sector ETFs resemble those with individual stocks. For brevity, we discuss the findings with respect to individual stocks only.

Table 5: Unconventional monetary policy announcements, systemic cojumps and crashes

Dates	Time	Type	Description of event	G2011	W2012	SCOJ-stat	SCOJ	SCRA-stat	SCRA	RV ratio	DRV ratio
2008-11-25	8:15	QE1	FOMC statement – Expansion of QE. Initial LSAP announcement. The Fed announces purchases of $100 billion in GSE debt and up to 500 billion in MBS. Creation of the Term Asset-Backed Security Loan Facility (TALF)	-22	0.75	NA	NA	NA	NA	NA	NA
2008-12-01	13:45	QE1	Bernanke Speech – Expansion of QE. Chairman Bernanke mentions that the Fed could purchase long-term Treasuries.	-19	0.84	5.24	22	4.06	20	1.41	1.44
2008-12-16	14:15	QE1	FOMC statement – Expansion of QE. The FOMC "evaluates" the potential benefits of purchasing longer-term Treasury securities. Also FED funds target rate reduced to the range 0- 0.25	-26	2.22	**(11.80)**	22	**(7.92)**	22	2.78	2.86
2009-01-28	14:15	QE1	FOMC statement – The FOMC disappointed markets by failing to actually expand asset purchases, although it said that it stood ready to do so. As a result, yields rose.	14	-0.23	8.35	22	6.09	22	2.27	2.45
2009-03-18	14:15	QE1	FOMC statement – Expansion of QE. The Fed will purchase an additional $750 billion in agency MBS and an additional $100 billion in Agency Debt. Moreover, the FOMC decided to purchase up to $300 billion of longer-term Treasury securities over the following six months.	-47	3.41	**(11.05)**	22	**(7.78)**	22	2.53	2.45
2009-08-12	14:15	QE1	FOMC statement – Phase out of QE. The Fed will slow the pace of the LSAP by purchasing the full amount by the end of October instead of mid- September.	5	0.15	5.57	22	4.23	21	2.11	2.30
2009-09-23	14:15	QE1	FOMC statement – Phase out of QE. The Fed will slow the purchases of agency MBS and agency debt, finishing the purchases by the end of 2010Q1. Treasury purchases will still be finished by October 2009.	-3	0.85	5.14	21	3.73	20	2.23	2.26
2009-11-04	14:15	QE1	FOMC statement– Phase out of QE. The amount of agency debt will be halted at $175 billion, instead of $200 billion.	6	0.12	6.52	22	4.38	20	2.40	2.27
2010-08-10	14:15	QE2	FOMC statement – Expansion of QE. The Fed will reinvest principal payments from agency debt and agency mortgage-backed securities in longer-term Treasury securities. Holdings of Treasury securities will be rolled over as they mature.	NA	0.57	5.85	22	4.14	22	2.62	2.55
2010-08-27	10:00	QE2	Bernanke speech – Expansion of QE. Bernanke mentions potential policy options for further easing, including additional purchases of long term securities.	NA	-0.83	NA	NA	NA	NA	NA	NA
2010-10-15	14:15	QE2	Bernanke speech – Expansion of QE. The Fed is prepared to provide additional accommodation if needed to support the economic recovery.	NA	-0.21	[**1.88**]	8	[**1.01**]	3	1.32	1.26
2010-11-03	14:15	QE2	FOMC statement – Expansion of QE. The Fed will purchase a further $600 billion of longer-term Treasury securities by the end of the second quarter of 2011, a pace of about $75 billion per month.	NA	-0.05	5.55	22	3.81	22	2.37	2.11

Notes: The table reports the detected systemic cojumps (SCOJ) and crashes (SCRA), conditional on the timing of Fed's QE announcements between 2008 and 2010. We apply our testing procedures by using the list of announcements considered in Fratzscher et al. (2018). These QE announcements are related to the first and second LSAP programs of the Fed. Fratzscher et al. (2018) consider twelve announcements in their analysis. To avoid timing problem, we discard two announcements from their list because these two QE announcements are released outside the trading hours of our stocks data. The table reports the release date, time of the event, announcement type (QE1 or QE2), the type of the event and the description of the event. "G2011" and "W2011" denote the estimated impact in Gagnon et al. (2011) and Wright (2012), respectively. In addition to the detected number of systemic cojumps and crashes, we further present the values of the corresponding test statistics, pre-/post-event realized volatility ratio (RV ratio) and pre-/post-event downside realized volatility ratio (DRV ratio). The table reports the two largest and smallest values of test statistics in parenthesis and square brackets, respectively.

QE announcements (SCOJ-stat). Individual stocks co-crash immediately in response to these two events (i.e., SCRA-stats of 7.92 and 7.78, respectively).

Bernanke's speech of October 15, 2010 (penultimate row) has the weakest systemic effect of all events in Table 5. The cross-sectional averages of the SCOJ and SCRA statistics for this QE event are 1.88 and 1.01, respectively, the lowest among all statistics while realized volatility changes little (news-driven RV and DRV ratios in Table 5).

To facilitate comparison of jump statistics and volatility across the 10 events, Figure 3 plots the SCOJ and SCRA test statistics, the RVOL and downside RVOL for each of the 22 stocks for each of the ten events. Each line in the upper panels represents one type of test statistic for one event for each of the 22 stocks. For example, the blue line in the upper left panel shows the SCOJ statistics during event E2,

i.e., December 16, 2008, for each of the 22 stocks. Stock 20 has the largest SCOJ statistic for E2. The two critical QE events (blue and pink dashed lines labeled as E2 and E4) produce the largest jump and volatility statistics while Bernanke's October 15, 2010 speech (a green dashed line labeled E9) has a very small systemic impact. Comparing line post-E9 versus pre-E9 in the lower panels of the figure reveals that realized volatility remained almost unchanged following this speech. The evidence holds across assets, which supports the conjecture that Fed news is likely to be a common asset pricing factor.

Figure 3: Unconventional monetary policy, realized volatility and systemic cojumps

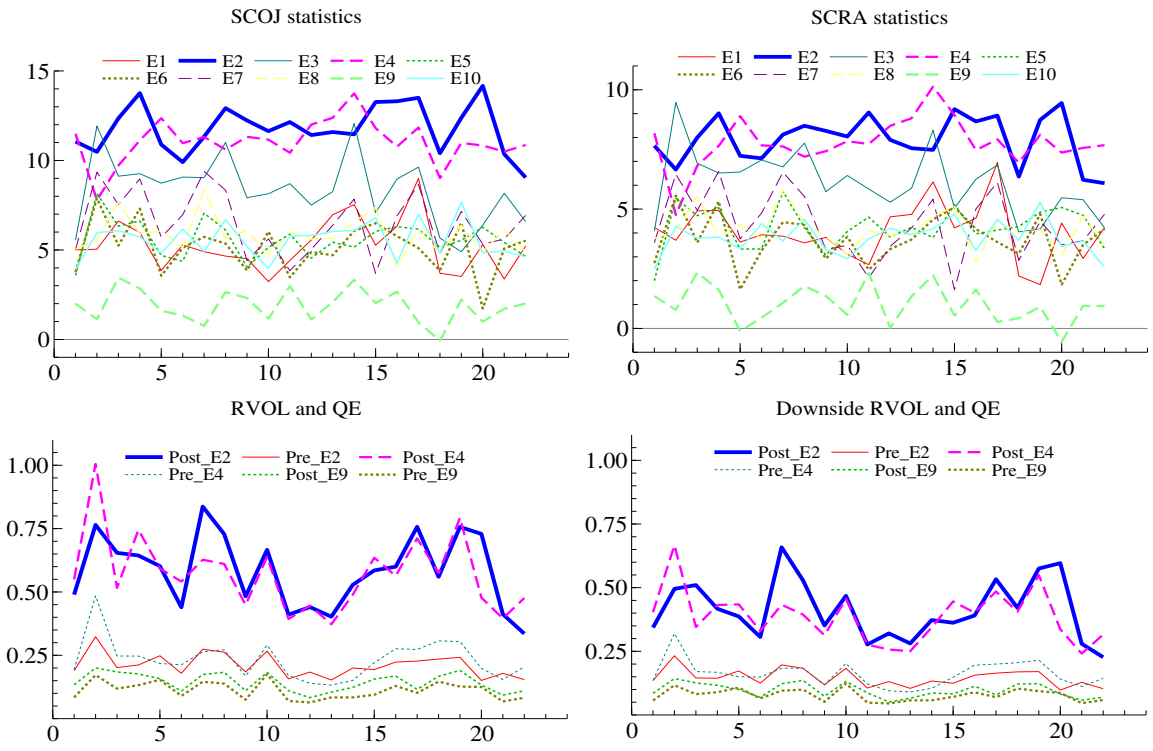

Notes: The figure shows the value of the computed test statistics of systemic cojumps (SCOJ) and crashes (SCRA), conditional on the timing of Fed's QE announcements. We apply our testing procedures by using the list of announcements considered in Fratzscher et al. (2018) (see Table 1 therein). These QE announcements are related to the first and second LSAP programs of the Fed. Fratzscher et al. (2018) consider twelve announcements in their analysis. To avoid timing problem, we discard two announcements from their list because these two QE announcements are released outside the trading hours of our stocks database, thus we use ten announcements (labeled as E1, E2,...,E10 in the upper panels of the figure). Table 5 describes these QE events and the results are based on the high-frequency data on 22 DJ stocks (see X-axis in all panels). In the lower panels, we display the values of realized volatility before and after the release of three events that are E2, E4 and E9 (pre-/post-RV). We compute pre-/post-event (downside) realized volatility by using only negative high-frequency returns (lower-right panel). Table 1 details the description of the Dow Jones stocks. The sample covers the periods from January 31, 2006 to January 30, 2019.

How do our measures of systemic cojumps correlate with measures of UMP surprises? The UMP-

driven systemic tail risk patterns corroborate those revealed by Gagnon et al. (2011) and Wright (2012). The two events for which we find the strongest systemic response, i.e., December 16, 2008 and March 18, 2009, generate the largest impact according to the estimates of Gagnon et al. (2011) and Wright (2012) (third and fifth lines in the table). There are some differences with respect to the features of least influential UMP events, however. For instance, the Wright surprise for November 3, 2010 FOMC statement is slightly negative (contractionary) and very weak (-0.05). Our test, however, suggests that this event has non-negligible influence, as all 22 individual stocks cojump downward in response to news. Other examples of such events include the announcements of January 28, 2009, August 12, 2009, and November 4, 2009, with Wright estimates of -0.23, 0.15 and 0.12, respectively. In contrast, these events create strong systemic cojumps (SCOJ, SCOJ-stat, SCRA, SCRA-stat) and substantial increases in downside ("bad") realized volatility (see DRV ratio in Table 5). These differences with Wright (2012) and Gagnon et al. (2011) are very likely due to the fact that we exploit the information in the cross-section, rather than in a time series of bond yields or a stock index.

Table 6: Third round of quantitative easing announcements, systemic cojumps and crashes

Dates	Time	Type	Description of event	SCOJ-Stat	SCOJ	SCRA-Stat	SCRA	RV ratio	DRV ratio
2012-09-13	1230	QE3	QE3 announced: Fed will purchase $40 billion of MBS per month as long as "the outlook for the labor market does not improve substantially... in the context of price stability." FOMC expects low rates "at least through mid-2015."	3.81	18	2.50	11	2.04	1.88
2012-12-12	1230	QE3	QE3 expanded: Fed will purchase $45 billion of long-term Treasuries per month but will no longer sterilize purchases through the sale of short-term Treasuries. FOMC expects low rates to be appropriate while unemployment is above 6.5 percent, and inflation is forecast below 2.5 percent.	1.35	1	0.71	0	1.32	1.27
2013-06-19	1400	QE3	FOMC will purchase "additional agency mortgage-backed securities at a pace of $40 billion per month and longer-term Treasury securities at a pace of $45 billion per month." Statement indicates no funds target increases in 2013.	5.89	22	4.42	21	2.92	3.13
2013-12-18	1400	QE3	Cut monthly purchases of MBS and Treasuries to $35 billion and $40 billion. Unemployment lift-off threshold of 6.5 % abandoned.	5.25	22	3.17	15	2.67	2.79
2014-01-29	1400	QE3	Cut monthly purchases of MBS and Treasuries to $30 billion and $35 billion.	4.51	20	3.14	15	2.19	2.16
2014-03-19	1400	QE3	Cut monthly purchases of MBS and Treasuries to $25 billion and $30 billion; Expand the information assessed in determining lift-off date.	4.49	21	3.52	16	2.47	2.66
2014-04-30	1400	QE3	Cut monthly purchases of MBS and Treasuries to $20 billion and $25 billion.	2.78	16	1.88	3	1.83	1.78
2014-06-18	1400	QE3	Cut monthly purchases of MBS and Treasuries to $15 billion and $20 billion.	3.37	15	2.24	6	2.06	1.97
2014-07-30	1400	QE3	Cut monthly purchases of MBS and Treasuries to $10 billion and $15 billion.	2.61	15	1.96	4	1.87	2.15
2014-09-17	1400	QE3	Cut monthly purchases of MBS and Treasuries to $5 billion and $10 billion	3.54	19	2.57	11	2.17	2.15
2014-10-29	1400	QE3	End of QE	3.74	19	2.75	13	2.11	2.12

Notes: The table reports the detected systemic cojumps (SCOJ) and crashes (SCRA), conditional on the timing of Fed's QE announcements during the QE3 period. We apply our testing procedures by using the list of announcements in the table (eleven events). The table reports the release date, time of the event, announcement type (QE3), the type of the event and the description of the event. In addition to the detected number of systemic cojumps and crashes, we further present the values of the corresponding test statistics, pre-/post-event realized volatility ratio (RV ratio) and pre-/post-event downside realized volatility ratio (DRV ratio).

We complete our analysis by investigating the effects of UMP announcements on cross-asset tail risk during QE3. Table 6 reports the results based on 11 UMP announcements between September 13, 2012 and October 29, 2014 (first column). In line with the QE1 and QE2 results, there is strong evidence of systemic (simultaneous) cojumps: QE3 announcements produce many stock price cojumps. The tail reaction to QE3 news is relatively weak, however, compared to reactions to QE1 and QE2 news. The average tail risk score (i.e., the average SCOJ-stat) across events during QE3 is around 3.76, which is lower than that during QE1 and QE2 (6.69, average SCOJ-stat, Table 5). During QE3, the "taper tantrum" of June 19, 2013 creates the most severe tail reaction with a SCOJ-stat of 5.89, and the least influential news is released on December 12, 2012 with a SCOJ-stat of 1.35.

Having assessed the UMP events during each phase of QE, we next discuss the use of our test statistics to measure systemic tail risk.

7.5 News-Driven Systemic Tail Risk Indicator

Traders and policymakers want to know how events change tail risk. We can construct a systemic risk indicator with our test statistics as follows: We first apply our tests to pre- and post-FOMC (high-frequency) data on the stocks and ETFs to identify the systemic cojumps/crashes for each event. We then calculate the cross-sectional averages of the standardized test statistics from the estimated jump intensities. For each event, we measure news-driven systemic risk with the product of that average test statistic and the fraction of detected systemic cojumps.

The lower panel of Figure 4 displays the tail risk scores over time, for each of the 22 individual Dow Jones stocks. The average market stress (thick solid line) tends to rise during the periods of global financial crisis (2007-2008) and decreases after 2009. Market movements are relatively *sensitive* to the FOMC announcements during 2008Q4-2009Q1. FOMC decisions generate relatively little market tension from 2010 until the first quarter of 2011, but tail risk scores dramatically increase in the second half of 2011, and even exceed the levels of late 2008, during which Lehman Brothers collapsed. The three surprise factors (target, path, and Wright surprise) fail to capture the spike in the market stress in 2011 (upper panel). FOMC decisions also generated elevated market movements during the runup to the liftoff from zero short rates in late 2015 and near the end of the tightening cycle in December 2018. None of the three benchmark shock factor series exhibit that high level of policy-driven realized tail risk. The risk scores

Figure 4: News-driven tail risk scores based on Dow Jones stocks

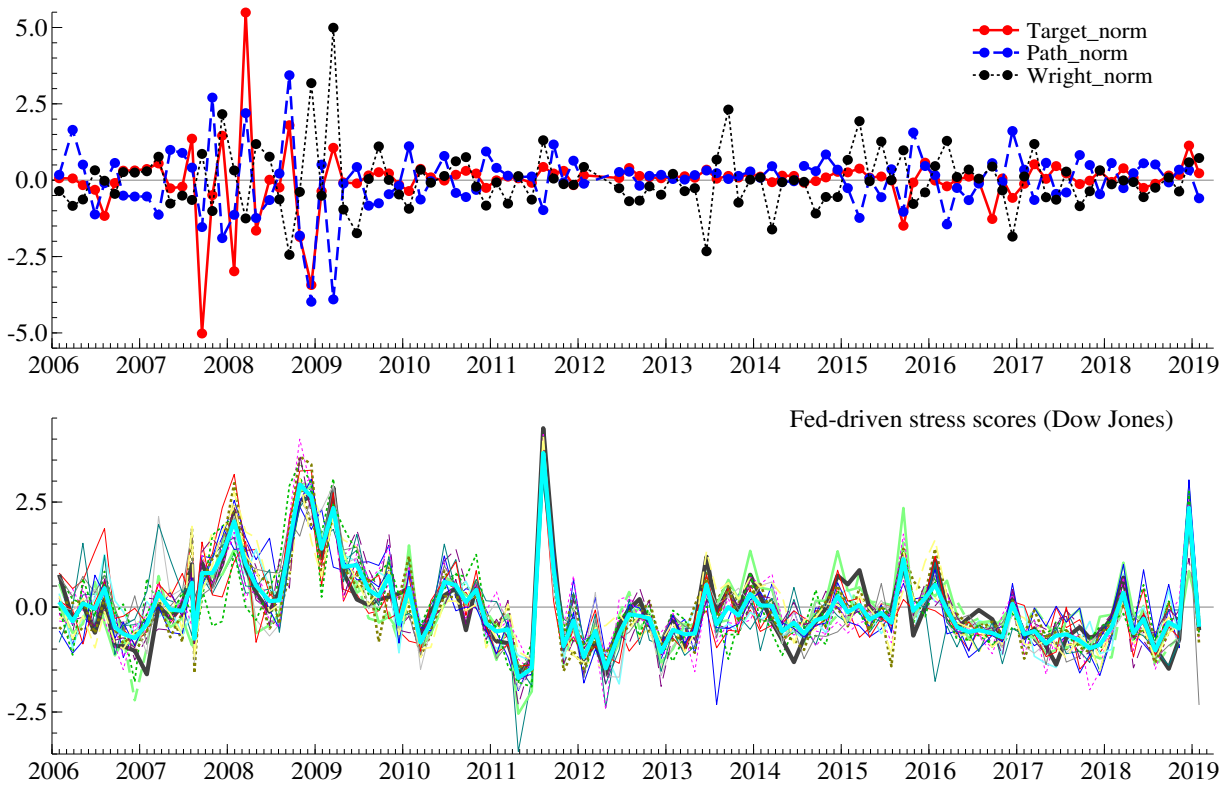

Notes: The figure illustrates the estimated monetary policy shocks (upper panel) and news-driven realized tail risk (RS) scores (lower panel) of each of the 22 Dow Jones stocks in our sample. The RS scores are the standardized test statistics of each Dow Jones constituent for each FOMC news announcement. In the lower panel, the light blue solid line is the cross-sectional average tail risk. The sample covers January 31, 2006 to January 30, 2019, and contains 106 FOMC policy announcements.

extracted from sector ETFs are similar to those of individual stocks.[21]

In the next sections, we ask whether this measure of Fed-driven systemic tail risk explains the pre-FOMC drift and variance risk premia.

7.6 Fed-Driven Systemic Tail Risk and Pre-FOMC Announcement Drift

Asset pricing theory predicts that investors should demand higher returns as compensation for holding undiversifiable risk. In the context of the capital asset pricing model (CAPM), for instance, covariance with market returns determines expected stock returns. However, Lucca and Moench (2015) (henceforth LM) show that stocks earned significant excess returns in the 24 hours before the release of the FOMC

[21] See Figure S.2 in our Supplementary Appendix.

statements, but not after. This anomaly has been difficult to explain as it is not obviously related to any risk. We revisit the evidence on pre-FOMC drift and conjecture that systemic tail risk from the *previous* FOMC meeting might predict pre-FOMC drift. Investors may expect compensation to hold stocks immediately prior to the next meeting if the Fed's previous decision at time t–1 produced a volatile market with high tail risk.

In investigating whether volatility and/or tail risk predicts FOMC drift, we must consider time variation in the pre-FOMC drift and in FOMC procedures, however. The original LM sample extended from 1994 through March 2011, but the pre-FOMC drift is only predominantly positive through mid-2010. Starting in 2011, the drift became predominantly negative through 2018. So, there is time variation in the pre-FOMC drift. Time variation in FOMC procedures might also affect reactions to FOMC volatility. Starting in April 2011, the FOMC started to hold press conferences, which were held every other meeting until 2019, when the FOMC began to hold them every meeting.[22]

To account for these changes in the data generating processes, we allow for changes in the predictive coefficients after 2010 and for differences in predictive coefficients for meetings that had press conferences. The following specification allows for a break in coefficients at the time that the LM drift starts to be persistently negative, in January 2011 and for different coefficients for meetings with/without press conferences (PC).

$$r_t^{(\text{pre})} = \beta_0 + \beta_1 X_{t-1} I(t < 2011) + \beta_2 X_{t-1} I(t > 2010 \ \& \ PC) + \beta_3 X_{t-1} I(t > 2010 \ \& \ \text{no } PC) + \epsilon_t, \quad (10)$$

where t is the date of the FOMC news release, $r_t^{(\text{pre})}$ is the cumulative pre-FOMC return, X_{t-1} is one of four risk measures from the previous FOMC meeting, and $I(t < 2011)$, $I(t > 2010 \ \& \ PC)$, and $I(t > 2010 \ \& \ \text{no } PC)$ are indicator functions that respectively take the value one for observations before 2011, observations after 2010 with a press conference, and observations after 2010 without a press conference.

We assess the impact of four measures of lagged tail risk on pre-FOMC cumulative returns: the lag of the log of realized volatility, the lagged realized tail risk indicator (TR_{t-1}), lagged systemic tail risk indicator (STR_{t-1}), and the fraction of assets that cojumped at the previous FOMC announcement ($SCOJ_{t-1}$). Realized volatility includes the total impact (i.e., both volatility and possibly single jumps) of

[22]The FOMC held press conferences at the April, June, and November 2011 meetings, and at the January, April, June, September, and December 2012 meetings. From 2013 through 2018, the FOMC held press conferences at the March, June, September, and December meetings.

the announcements but not the systemic component embedded in jump intensity and tails. TR_{t-1} is the lagged cross-sectional median of systemic cojump test statistics computed conditional on the FOMC news event, and STR_{t-1} is the weighted version of the TR_{t-1}, based on the fraction of stocks that previously cojumped as the weight (i.e., $SCOJ_{t-1}$). We interpret STR as a gauge of Fed-driven systemic tail risk. To compare the coefficients more easily across equations, we scaled the dependent variable, $r_t^{(\text{pre})}$ and the four risk measures (X_{t-1}) to have unit variance. That is, a coefficient describes how many standard deviations of pre-FOMC drift occur due to a one standard deviation increase in each risk measure. We emphasize that these predictors are lagged about 6 weeks before the stock drift they predict; they are not contemporaneous with the dependent variable, i.e., pre-FOMC drift.

The top panel of Table 7 reports positive, statistically significant estimates of the coefficients β_1 and β_3 from Equation (10). The estimates of β_1 and β_3 are of very similar magnitudes for each of the four risk measures and Wald tests cannot reject the restriction that $\beta_1 = \beta_3$. The Wald tests are in the last rows of Table 7). In other words, the risk factors are strong predictors of pre-FOMC drift in the original LM sample, and again in the post-2010 sample, for meetings without press conferences, but not for other meetings. We cannot reject that the risk factors predict the same FOMC drift either for the pre-2011 sample or the post-2010 sample for meetings without press conferences. One cannot reject that the risk factors fail to predict post-2010 pre-FOMC drift at meetings with press conferences. That is, we cannot reject that $\widehat{\beta}_2$ equals zero.

Because Wald tests cannot reject the restriction that $\beta_1 = \beta_3$ and theory provides no reason that these coefficients should differ, we impose that restriction and estimate the following regression:

$$r_t^{(\text{pre})} = \beta_0 + \beta_1 X_{t-1} I(t < 2011 \text{ or } (t > 2010 \ \& \text{ no } PC)) + \beta_2 X_{t-1} I(t > 2010 \ \& \ PC) + \epsilon_t. \tag{11}$$

The lower panel of Table 7 strengthens the evidence that policy-induced tail risk predicts pre-FOMC returns. The $\widehat{\beta}_1$ coefficients are highly statistically significant for all four lagged risk measures and financially relevant. A one standard deviation rise to a risk measure increases the pre-FOMC returns by about 0.28 to 0.38 standard deviations. In both the upper and lower panels, the best fit comes from the TR_{t-1} risk measure, and the weakest results come from the fraction of cojumps ($SCOJ$). All four risk measures produce fairly similar results, however.

Table 7: Lagged regressions for pre-FOMC announcement returns

Panel A. Unrestricted	$\log(RV_{t-1}^{post})$	TR_{t-1}	STR_{t-1}	$SCOJ_{t-1}$
X_{t-1} (pre-2011)	0.36	0.39	0.36	0.19
(t-stat)	(2.38)	(2.69)	(2.46)	(1.07)
X_{t-1} (post-2010/PC)	-0.01	-0.09	-0.12	0.02
(t-stat)	(-0.07)	(-0.42)	(-0.58)	(0.11)
X_{t-1} (post-2010/no PC)	0.40	0.38	0.33	0.35
(t-stat)	(2.12)	(2.20)	(1.82)	(2.11)
constant	-0.05	-0.06	-0.07	-0.02
(t-stat)	(-0.48)	(-0.62)	(-0.69)	(-0.18)
R^2	0.10	0.11	0.09	0.06
$\bar{R}^2$	0.08	0.09	0.07	0.03
F-stat	3.94	4.33	3.41	2.01
F-stat (p-value)	0.01	0.01	0.02	0.12
Wald stat, b1 = b3	0.03	0.00	0.02	0.43
Wald p-value	0.87	0.97	0.88	0.51

Panel B. Restricted	$\log(RV_{t-1}^{post})$	TR_{t-1}	STR_{t-1}	$SCOJ_{t-1}$
X_{t-1} (pre-2011/post-2010/no PC)	0.38	0.39	0.35	0.28
(t-stat)	(3.41)	(3.57)	(3.15)	(2.34)
X_{t-1} (post-2010 PC)	-0.02	-0.09	-0.12	0.01
(t-stat)	(-0.10)	(-0.42)	(-0.57)	(0.04)
constant	-0.06	-0.06	-0.07	-0.05
(t-stat)	(-0.62)	(-0.65)	(-0.69)	(-0.44)
R^2	0.10	0.11	0.09	0.05
$\bar{R}^2$	0.08	0.09	0.07	0.02
F-stat	5.95	6.56	5.16	2.82
F-stat (p-value)	0.00	0.00	0.01	0.06

Notes: The table reports results of regressing pre-FOMC high-frequency returns on tail risk measures, as in Equation (10). These independent variables include the lagged realized volatility ($\log(RV_{t-1}^{post})$), lagged realized tail risk indicator (TR_{t-1}), lagged systemic tail risk indicator (STR_{t-1}) and the fraction of assets that cojump together (systemically) at the previous event's testing time $(t-1)$ ($SCOJ_{t-1}$). Panel A reports the unrestricted version of Equation (10) while Panel B restricts $\beta_1 = \beta_3$. The results are based on the high-frequency data on 22 stocks listed in the Dow Jones index. Table 1 details the description of the Dow Jones stocks. The sample covers the periods from December 16, 2008 to January 30, 2019, and contains 82 FOMC policy announcements. Structural instability prompts us to omit the first 24 observations in the sample.

7.7 The Impact of Fed-Driven Systemic Tail Risk on Variance Risk Premia

Finally, we investigate whether Fed-driven systemic tail risk impacts variance risk premia. If Fed-driven systemic tail risk matters, then investors may demand compensation for exposure to this form of risk.

The variance risk premium (VRP) at time t is the difference between the risk-neutral (ex-ante) expectation and the physical (statistical) expectation of an asset return variance over the time interval [t, t+1].

That is,

$$VRP_t \equiv \mathrm{E}_t^Q(\mathrm{Var}_{t,t+1}) - \mathrm{E}_t^P(\mathrm{Var}_{t,t+1}), \tag{12}$$

where the asset return variance $\mathrm{Var}_{t,t+1}$ corresponds to, for instance, quadratic variation (see e.g., Caporin et al., 2017). We follow the literature and use a proxy for the latent VRP_t.

$$\widehat{VRP_t} \equiv \mathrm{IV}_{t,t+1} - \mathrm{RV}_{t-1,t}, \tag{13}$$

where $\mathrm{IV}_{t,t+1}$ and $\mathrm{RV}_{t-1,t}$ are the implied variance and lagged realized variance at time t, respectively. The squared VIX index approximates the implied variance $\mathrm{IV}_{t,t+1}$ so that

$$\widehat{VRP_t} \equiv \mathrm{VIX}_{t,t+1}^2 - \mathrm{RV}_{t-1,t}, \tag{14}$$

and the realized variance is computed in a standard way as the sum of squared intradaily returns over a day. To assess the effects of our systemic tail risk indicator on variance risk premia, we estimate the following regression specification:

$$\widehat{VRP_t} = \theta_0 + \theta_1 \widehat{VRP_{t-1}} + \theta_{STR} STR_t + \epsilon_t, \tag{15}$$

where STR_t is our systemic tail risk (STR) indicator associated with the FOMC announcements at time t and ϵ_t is the error term. If FOMC announcements amplify tail risk, investors may demand compensation for bearing such systemic tail risk. We thus expect a positive estimated coefficient, θ_{STR}.

We begin our analysis by investigating the structural stability of Equation (15). Structural break test statistics for Equation (15) are significant at any conventional level around December 2008, which was the break between the Fed's use of conventional and purely unconventional monetary policy.[23] We therefore began our sample in December 2008, which left 82 observations.

We consider two models of the variance risk premia starting in December 2008. The first is Equation (15). The second model follows the logic used in the construction of Table 7 and allows for 3 separate coefficients for the lagged VRP and lagged TR variables: (1) pre-2011 sample; (2) post-2010 meetings with press conferences; (3) post-2010 meetings without press conferences. Equation (16) below shows the

[23] The first Federal Reserve unconventional asset purchase announcement was November 25, 2008, while the FOMC meeting on December 16, 2008 would feature the last change in the federal funds target—down to a 0-to-25 bp range—until it was raised in 2015.

functional form of the second model.

$$\begin{aligned}\widehat{VRP_t} = \theta_0 + \theta_1 \widehat{VRP_{t-1}} I(t < 2011) + \theta_2 \widehat{VRP_{t-1}} I(t > 2010 \ \& \ PC) + \theta_3 \widehat{VRP_{t-1}} I(t > 2010 \ \& \text{ no } PC) \\ + \theta_4 \widehat{STR_{t-1}} I(t < 2011) + \theta_5 \widehat{STR_{t-1}} I(t > 2010 \ \& \ PC) + \theta_6 \widehat{STR_{t-1}} I(t > 2010 \ \& \text{ no } PC) + \epsilon_t.\end{aligned} \tag{16}$$

We estimated both sets of models and found mixed evidence about the better fit. The AIC selected the second (larger) model for each of the 7 specifications while the SC selected the second (larger) model for 3 of the 7 specifications, although one specification was nearly a tie. The mixed evidence with respect to the better model fit prompts us to present results from both models.

Table 8: The impact of systemic tail risk on variance risk premia

	1	2	3	4	5	6	7
VRP_{t-1}	0.098**	0.172**	0.151**	0.169**	0.165**	0.175**	0.167**
(s.e.)	(0.060)	(0.053)	(0.054)	(0.054)	(0.055)	(0.052)	(0.054)
TR_{t-1}		0.306**					
(s.e.)		(0.057)					
STR_{t-1}			0.276**				
(s.e.)			(0.058)				
LTR_{t-1}				0.295**			
(s.e.)				(0.058)			
$LSTR_{t-1}$					0.279**		
(s.e.)					(0.060)		
RTR_{t-1}						0.318**	
(s.e.)						(0.056)	
$RSTR_{t-1}$							0.298**
(s.e.)							(0.059)
constant	0.138**	0.158**	0.155**	0.157**	0.151**	0.160**	0.157**
(s.e.)	(0.066)	(0.057)	(0.059)	(0.058)	(0.059)	(0.056)	(0.058)
R^2	0.034	0.299	0.252	0.281	0.245	0.317	0.272
$\bar{R}^2$	0.022	0.281	0.233	0.263	0.226	0.300	0.254
F-stat	2.79	16.86	13.30	15.45	12.83	18.35	14.75
p-value	0.099	0.000	0.000	0.000	0.000	0.000	0.000
SC	-77.47	-98.37	-93.01	-96.29	-92.29	-100.51	-95.24
AIC	-82.28	-105.59	-100.23	-103.51	-99.51	-107.73	-102.46

Notes: The table reports the results of estimation of Equation (15). We regress the time series of estimated (standardized) VRP on the lagged tail risk (TR) and systemic tail risk (STR) indicators, controlling for the autoregressive effect (Equation (15)). The table presents the estimated regression coefficients for both tails, based on the indicators for left tails (LTR, LSTR) and right tails (RTR, RSTR), respectively. The TR indicator is the cross-sectional median of systemic co-jump test statistics computed conditional on the FOMC news events. The STR indicator weights the TR indicator by the fraction of stocks that systemically cojump for a given event. We obtain the left and right tail indicators, respectively, by using the jump intensity estimates based on the negative and positive high-frequency returns. The sample covers the periods from January 31, 2006 to January 30, 2019. The table reports the coefficient estimates and standard errors (s.e.) in parentheses. ** denotes statistical significance at 5%.

Table 8 presents the results from the simpler model (Equation (15)) of the VRP regressions when we construct our regressors using both tails (columns 2 and 3) or left and right tails (columns 4 and 5 and 6 and 7, respectively). The estimated coefficients of the tail risk (TR) and systemic tail risk (STR) indicators are positive and very significant (0.306, 0.276, respectively) in columns 2 and 3, even after we control for the lagged VRP effect (0.172/0.151). The model including our systemic tail risk indicator has a high R^2 of 25.2% (column (3)). Upside and downside tail risk components have similar effects; the estimated coefficients are quite similar (in Panels B and C). The standardized systemic tail risk indicators have much larger coefficients than the standardized lagged VRP in all models.

Table 9 reports the results from the more elaborate model that allows for different treatment of data before and after 2011 and different treatment of press conferences. The more flexible model delivers somewhat different inference. First, the coefficients on the standardized regressors are generally much larger than in the first model. Second, the coefficient on the lagged VRP is positive and significant before 2011—that is, before the LM drift changed—but negative and significant after the start of 2011 for dates with no press conference. Third, the coefficients on the TR variables are all positive for the meetings before the start of 2011 and after the start of 2011 without press conferences. These two sets of TR coefficients are similarly sized between these subsamples. The coefficients from symmetric, left-hand and right-hand TR are very similar.

In summary, the VRP regression results in Table 9 reveal that Fed-driven systemic tail risk substantially increases risk premia prior to the start of 2011 and during meetings without press conferences after the start of that year. This finding implies that the Fed-driven, extreme-downside risk is priced in options, particularly when there is no press conference. During these periods, investors demand compensation for bearing systemic cojump tail risk triggered by monetary policy announcements.

8 Extensions and Robustness Checks

We carry out several robustness checks and extensions. First, we assess whether or not macroeconomic news announcements create systemic tail risk. Second, we examine whether the sign of monetary shocks influences tail effects. Third, we evaluate the tail risk patterns for sector ETFs. Fourth, we consider the threshold selection (i.e., fixed versus time-varying) for applying the tests and compare our measure with alternative approaches. Fifth, we compare the empirical rejection rates of the bias-corrected test with

Table 9: Systemic tail risk effects on variance risk premia for meetings with and without press conferences

	1	2	3	4	5	6	7
VRP_{t-1} (pre-2011)	0.166**	0.258**	0.237**	0.259**	0.252**	0.256**	0.246**
(s.e.)	(0.058)	(0.054)	(0.054)	(0.054)	(0.055)	(0.053)	(0.054)
VRP_{t-1} (post-2010/PC)	-0.018	-0.017	-0.015	-0.017	-0.005	-0.018	-0.013
(s.e.)	(0.181)	(0.154)	(0.160)	(0.155)	(0.160)	(0.152)	(0.158)
VRP_{t-1} (post-2010/no PC)	-0.938**	-0.489**	-0.655**	-0.525**	-0.496**	-0.470**	-0.524**
(s.e.)	(0.253)	(0.262)	(0.259)	(0.260)	(0.288)	(0.258)	(0.277)
TR_{t-1} (pre-2011)		0.408**					
(s.e.)		(0.091)					
TR_{t-1} (post-2010/PC)		0.012					
(s.e.)		(0.103)					
TR_{t-1} (post-2010/no PC)		0.315**					
(s.e.)		(0.101)					
STR_{t-1} (pre-2011)			0.399**				
(s.e.)			(0.093)				
STR_{t-1} (post-2010/PC)			0.001				
(s.e.)			(0.108)				
STR_{t-1} (post-2010/no PC)			0.232**				
(s.e.)			(0.102)				
LTR_{t-1} (pre-2011)				0.414**			
(s.e.)				(0.093)			
LTR_{t-1} (post-2010/PC)				0.006			
(s.e.)				(0.099)			
LTR_{t-1} (post-2010/no PC)				0.303**			
(s.e.)				(0.102)			
$LSTR_{t-1}$ (pre-2011)					0.368**		
(s.e.)					(0.087)		
$LSTR_{t-1}$ (post-2010/PC)					-0.045		
(s.e.)					(0.110)		
$LSTR_{t-1}$ (post-2010/no PC)					0.309**		
(s.e.)					(0.124)		
RTR_{t-1} (pre-2011)						0.414**	
(s.e.)						(0.091)	
RTR_{t-1} (post-2010/PC)						0.017	
(s.e.)						(0.105)	
RTR_{t-1} (post-2010/no PC)						0.323**	
(s.e.)						(0.097)	
$RSTR_{t-1}$ (pre-2011)							0.383**
(s.e.)							(0.090)
$RSTR_{t-1}$ (post-2010/PC)							-0.022
(s.e.)							(0.115)
$RSTR_{t-1}$ (post-2010/no PC)							0.291**
(s.e.)							(0.113)
constant	0.122**	0.083	0.067	0.083	0.085	0.085	0.077
(s.e.)	(0.060)	(0.058)	(0.061)	(0.059)	(0.060)	(0.058)	(0.061)
R^2	0.223	0.463	0.424	0.458	0.429	0.473	0.432
$\bar{R}^2$	0.193	0.420	0.378	0.415	0.383	0.430	0.386
F-stat	7.47	10.79	9.20	10.57	9.39	11.20	9.50
p-value	0.000	0.000	0.000	0.000	0.000	0.000	0.000
SC	-84.48	-98.35	-92.55	-97.56	-93.28	-99.80	-93.69
AIC	-94.10	-115.19	-109.39	-114.41	-110.13	-116.65	-110.54

Notes: The table reports the results of estimation of Equation (16). We regress the time series of estimated (standardized) VRP on the lagged tail risk (TR) and systemic tail risk (STR) indicators, controlling for the autoregressive effect (Equation (16)). Coefficients are allowed to differ before and after the start of 2011. After the start of 2011, coefficients are allowed to differ for meetings with and without press conferences. The table presents the estimated regression coefficients for both tails, based on the indicators for left tails (LTR, LSTR) and right tails (RTR, RSTR), respectively. The TR indicator is the cross-sectional median of systemic cojump test statistics computed conditional on the FOMC news events. The STR indicator weights the TR indicator by the fraction of stocks that systemically cojump for a given event. We obtain the left and right tail indicators, respectively, by using the jump intensity estimates based on the negative and positive high-frequency returns. The table reports the coefficient estimates and standard errors (s.e.) in parentheses. ** denotes statistical significance at 5%.

the uncorrected basic version. Finally, we show that our STR and LSTR measures detect major tail-risk events in a manner consistent with other measures. For brevity, we only discuss the main robustness

checks and extensions but our Supplementary Online Appendix contains full results.

Macroeconomic News Announcements. We obtain the time stamps of several important types of macro news events from Bloomberg Analytics, then implement our approach by using these scheduled macroeconomic news announcements.

The systemic response of stocks to the release of macro events appears to be very weak, producing test statistics around 2 in absolute terms, suggesting a modest reaction. Between years 2006 and 2012, the systemic effects of macroeconomic news announcements become more noticeable for ISM Manufacturing and New Home Sales. With controls for the multiple testing bias, however, we find no evidence of macro-driven systemic cojumps risk. In contrast, the systemic effects of FOMC events are very strong with test statistics around 10 and above. This analysis strongly corroborates the results of Bajgrowicz et al. (2016) in two respects. First, we confirm that the link between macro news and jumps is spurious. Second, because jumps and macro events are "disconnected", the risk ascribed to macro news could be diversifiable. Departing from the results of Bajgrowicz et al. (2016), however, we find that the jump impact of FOMC news is highly significant, non-spurious and systemic. FOMC announcements appear to convey more information about the exposure of investment strategies to tail risks than do macro releases.

Negative versus Positive Monetary Policy Shocks. Caporin et al. (2017) show that systemic cojumps driven by *good* FOMC news tend to *decrease* the variance risk premium. From a monetary policy perspective, the definition of good versus bad news may not be immediately clear and/or difficult to measure, however. We take an alternative route: we separate the FOMC events that create positive shocks from those that create negative shocks.[24] We find no clear evidence that systemic cojump risk are associated with *only* negative monetary policy shocks. Both positive and negative shocks of all three types contribute to systemic cojumps.

Sector ETFs and Systemic Tail Risk. We apply our approach to sector ETF portfolios to assess how systemic tail risk affects sector portfolio indices. We first compute realized volatility of each sector index before and after each FOMC announcement. For each sector index, post-FOMC realized volatility is higher than pre-FOMC realized volatility (see Figure S.1). In the second step, we generate the news-driven

[24]Recall that positive (negative) Wright shocks are expansionary (contractionary) while positive (negative) target and path shocks are contractionary (expansionary). The reason for this inconsistency in normalization is that Wright (2012) uses bond futures prices while Gürkaynak et al. (2005) worked with yields.

tail risk indicators—computed from standardized test statistics (Figure S.2). Systemic tail risk measures for the sectors vary similarly over time. This regularity is consistent with our results from individual stocks and suggests that sector rotation strategies may not diversify the tail risk due to Fed news.

Threshold Adjustment for Periodic Volatility. When asset prices jump simultaneously in response to FOMC announcements, diffusive volatility of each asset could also jump, making large diffusive movements appear to be price jumps. We employ a threshold adjustment to prevent this problem so that high levels of post-event volatility in the panel of assets will not be erroneously identified as systemic cojumps or crashes. Therefore, we adjust the post-announcement thresholds that separate systemic cojumps from diffusive volatility. That is, we generate two event-based thresholds: one value for the pre-event window and another for the post-event window. We confirm that larger values of the post-event threshold do not change the arrival times of systemic cojumps and crashes detected at high frequency.[25]

Bias-Corrected Test versus Basic Test. In our simulation study (see Appendix 5), we evaluate the power of our test and compare its finite-sample performance with the uncorrected (basic) version. We extend this evaluation by similarly analyzing the empirical rejection rates. Accordingly, we compare our proposed test based on the StepM procedure for bias correction (to prevent spurious detections) with the basic test without any correction. Table E.5 presents the summary statistics that indicate that the uncorrected version detects more systemic cojumps than the bias-corrected test (18.61 versus 12.77 for Dow Jones stocks and 6.49 versus 4.93 for sector ETFs, respectively). For all events, our StepM bias-corrected test detects 1354 jumps in Dow Jones stocks, while the uncorrected version detects 1973 jumps. We observe a similar pattern for sector ETFs (523 versus 688). These results demonstrate that bias produces spurious detections and an overestimate of tail risk.

Comparison with Alternative Tail Risk Measures. Dierkes et al. (2024) find that the option-implied tail risk measure of Bollerslev and Todorov (2011) ($BT11Q$) performs best in predicting the tail events. While we leave an in-depth analysis of the predictive performance of our tail risk measure for future research, we compare our ranking of tail risk events with the ranking generated by the $BT11Q$ approach along with the left tail risk measures of Bollerslev et al. (2015); Andersen et al. (2021) and Todorov and

[25] These findings and our implementation procedures are available upon request.

Zhang (2022).[26] Table S.3 indicates our STR and LSTR measures predict major tail-risk events, such as October 29, 2008, December 16, 2008, January 28, 2009, March 18, 2009, and August, 9, 2011, in a manner similar to other measures such as $BT11Q$ and LTV. This close relationship with $BT11Q$ approach implies that our approach is prone to *measurement error*, which is considered to be the main driver of the relative performance of tail risk measures.[27] Our measure complements existing tail risk measures and has the advantage of being adaptable to different contexts (e.g., asset classes, regions, or time horizons) and easy to compute, requiring only high-frequency data and event time stamps.

9 Concluding Remarks

It is well known that jumps in asset prices create idiosyncratic and systematic (tail) risk (e.g., Bégin et al., 2020; Pelger, 2020; Weller, 2019; Bollerslev et al., 2008, 2013). While the former concerns the behavior of individual asset prices, the latter involves the joint risk of security prices with the market index. Tail risk measurement matters for asset pricing, risk premia estimation, and diversification strategies.

We extend this line of research by studying systemic tail risk created by cojumps and news arrivals. Systemic tail risk implies cojumps in multiple assets, but not necessarily in the market index. Our methods identify systemic synchronized, multi-asset tail risk conditional on the arrival of events. We use this event-based approach to uncover the systemic effects of FOMC announcements on a panel of individual stocks and ETF portfolios: FOMC news is often associated with significant systemic jumps. The episodes of systemic tail risk occurred disproportionately during the Great Financial Crisis and its aftermath (2008-2010), but recur over the business cycle and coincide with large monetary policy surprises. The evidence suggests that diversifying jump risk is likely to be more difficult than previously thought, especially when the risk is associated with monetary policy news rather than macro news.

Our method generates systemic tail risk indicators with two useful properties. First, systemic tail risk seems to explain the variation in pre-FOMC announcement drift ahead of the upcoming Fed meeting. A one standard deviation increase in systemic tail risk raises pre-FOMC returns by about 0.33 standard deviations on average. In line with the discussion in Cieslak et al. (2019) regarding the Fed news premium, the stock market appears to price in the Fed-driven systemic tail risk that we quantify.

[26] We are grateful to Viktor Todorov and Fabian Hollstein for sharing the data on left tail variation, spot volatility index and $BT11Q$ measure, respectively.

[27] See Sections 1 and 6 in Dierkes et al. (2024) for a related discussion.

Second, Fed-driven systemic tail risk significantly increases variance risk premia. Investors demand compensation for bearing the systemic tail risk associated with Fed news during meetings *without* press conferences. We also show that our measure complements existing option-based tail risk measures, such as those developed in Todorov and Zhang (2022), Andersen et al. (2021), and Bollerslev and Todorov (2011), in identifying tail events.

Macroeconomic news announcements differ from FOMC announcements, however, in that they do not appear to create systemic tail risk, which supports the findings of Bajgrowicz et al. (2016). Therefore, understanding the role of macro news for management of tail risk will require further research.

References

Aït-Sahalia, Y., Cacho-Diaz, J., Laeven, R.J.A., 2015. Modeling financial contagion using mutually exciting jump processes. Journal of Financial Economics 117, 585–606.

Aït-Sahalia, Y., Jacod, J., 2009a. Estimating the degree of activity of jumps in high frequency data. The Annals of Statistics 37, 2202–2244.

Aït-Sahalia, Y., Jacod, J., 2009b. Testing for jumps in a discretely observed process. The Annals of Statistics 37, 184–222.

Aït-Sahalia, Y., Xiu, D., 2016. Increased correlation among asset classes: Are volatility or jumps to blame, or both? Journal of Econometrics 194, 205–219.

Amengual, D., Xiu, D., 2018. Resolution of policy uncertainty and sudden declines in volatility. Journal of Econometrics 203, 297–315.

Andersen, T.G., Bollerslev, T., Diebold, F.X., 2007. Roughing it up: Including jump components in the measurement, modelling and forecasting of return volatility. The Review of Economics and Statistics 89, 701–720.

Andersen, T.G., Fusari, N., Todorov, V., 2020. The pricing of tail risk and the equity premium: Evidence from international option markets. Journal of Business and Economic Statistics 38, 662–678.

Andersen, T.G., Todorov, V., Ubukata, M., 2021. Tail risk and return predictability for the Japanese equity market. Journal of Econometrics 222, 344–363.

Bajgrowicz, P., Scaillet, O., Treccani, A., 2016. Jumps in high-frequency data: Spurious detections, dynamics, and news. Management Science 62, 2149–2455.

Bandi, F.M., Renò, R., 2016. Price and volatility co-jumps. Journal of Financial Economics 119, 107–146.

Barndorff-Nielsen, O.E., Shepard, N., 2006. Econometrics of testing for jumps in financial economics using bipower variation. Journal of Financial Econometrics 4, 1–30.

Bates, D.S., 2019. How crashes develop: Intradaily volatility and crash evolution. The Journal of Finance 74, 193–238.

Bauer, M.D., Neely, C.J., 2014. International channels of the Fed's unconventional monetary policy. Journal of International Money and Finance 44, 24–46.

Bégin, J.F., Dorion, C., Gauthier, G., 2020. Idiosyncratic jump risk matters: Evidence from equity returns and options. The Review of Financial Studies 33, 155–211.

Bibinger, M., Neely, C.J., Winkelmann, L., 2019. Estimation of the discontinuous leverage effect: Evidence from the NASDAQ order book. Journal of Econometrics 209, 158–184.

Bibinger, T., Winkelmann, L., 2015. Econometrics of co-jumps in high-frequency data with noise. Journal of Econometrics 184, 361–378.

Bollerslev, T., Law, T.H., Tauchen, G., 2008. Risk, jumps, and diversification. Journal of Econometrics 144, 234–256.

Bollerslev, T., Li, J., Xue, Y., 2018. Volume, volatility, and public announcements. The Review of Economic Studies 85, 2005–2041.

Bollerslev, T., Todorov, V., 2011. Tails, fears and risk premia. The Journal of Finance 66, 2165–2211.

Bollerslev, T., Todorov, V., 2014. Time-varying jump tails. Journal of Econometrics 183, 168–180.

Bollerslev, T., Todorov, V., Li, S.Z., 2013. Jump tails, extreme dependencies and the distribution of stock returns. Journal of Econometrics 172, 307–324.

Bollerslev, T., Todorov, V., Xu, L., 2015. Tail risk premia and return predictability. Journal of Financial Economics 118, 113–134.

Boswijk, H.P., Laeven, R.J.A., Yang, X., 2018. Testing for self-excitation in jumps. Journal of Econometrics 203, 256–266.

Caporin, M., Kolokolov, A., Renò, R., 2017. Systemic co-jumps. Journal of Financial Economics 126, 563–591.

Chan, K., Bowman, R.G., Neely, C.J., 2017. Systematic cojumps, market component portfolios and scheduled macroeconomic announcements. Journal of Empirical Finance 43, 43–58.

Chordia, T., Sarkar, A., Subrahmanyam, A., 2005. An empirical analysis of stock and bond market liquidity. The Review of Financial Studies 18, 85–129.

Christensen, J.H.E., Rudebusch, G.D., 2012. The response of interest rates to U.S. and U.K. quantitative easing. The Economic Journal 122, F385–F414.

Cieslak, A., Morse, A., Vissing-Jorgensen, A., 2019. Stock returns over the FOMC cycle. The Journal of Finance 74, 2201–2248.

Cieslak, A., Schrimpf, A., 2019. Non-monetary news in central bank communication. Journal of International Economics 118, 293–315.

Corradi, V., Distaso, W., Fernandes, M., 2020. Testing for jump spillovers without testing for jumps. Journal of the American Statistical Association 115, 1214–1226.

Das, S.R., Uppal, R., 2005. Systemic risk and international portfolio choice. The Journal of Finance 59, 2809–2834.

Di Maggio, M., Kermani, A., Palmer, C.J., 2020. How quantitative easing works: Evidence on the refinancing channel. The Review of Economic Studies 87, 1498–1528.

Dierkes, M., Hollstein, F., Prokopczuk, M., Würsig, C.M., 2024. Measuring tail risk. Journal of Econometrics 241, 105769.

Dumitru, A.M., Urga, G., 2012. Identifying jumps in financial assets: A comparison between nonparametric jump tests. Journal of Business and Economic Statistics 30, 242–255.

Dungey, M., Erdemlioglu, D., Matei, M., Yang, X., 2018. Testing for mutually exciting jumps and financial flights in high frequency data. Journal of Econometrics 202, 18–44.

Dungey, M., Hvozdyk, L., 2012. Cojumping: Evidence from the US Treasury bond and futures markets. Journal of Banking and Finance 36, 1563–1575.

Erdemlioglu, D., Yang, X., 2022. News arrival, time-varying jump intensity, and realized volatility: Conditional testing approach. Journal of Financial Econometrics nbac015, 1–38.

Evans, K.P., 2011. Intraday jumps and US macroeconomic news announcements. Journal of Banking and Finance 35, 2511–2527.

Fawley, B.W., Neely, C.J., 2014. The evolution of federal reserve policy and the impact of monetary policy surprises on asset prices. Federal Reserve Bank of St. Louis Review 96, 73–109.

Fratzscher, M., Duca, M.L., Straub, R., 2018. On the international spillovers of US quantitative easing. The Economic Journal 128, 330–377.

Gagnon, J., Raskin, M., Remache, J., Sack, B., 2011. The financial market effects of the Federal Reserve's Large-Scale Asset Purchases. International Journal of Central Banking 7, 45–52.

Gilder, D., Shackleton, M.B., Taylor, S.J., 2014. Cojumps in stock prices: Empirical evidence. Journal of Banking and Finance 44, 443–459.

Gürkaynak, R.S., Sack, B., Swanson, E.T., 2005. Do actions speak louder than words? The response of asset prices to monetary policy actions and statements. International Journal of Central Banking 1, 55–93.

Hattori, M., Schrimpf, A., Sushko, V., 2016. The response of tail risk perceptions to unconventional monetary policy. American Economic Journal: Macroeconomics 8, 111–136.

Hayashi, F., Koeda, J., 2019. Exiting from quantitative easing. Quantitative Economics 3, 1069–1107.

Hill, B.M., 1975. A simple general approach to inference about the tail of a distribution. Annals of Statistics 3, 1163–1174.

Jacod, J., Klüppelberg, C., Müller, G., 2017. Testing for non-correlation between price and volatility jumps. Journal of Econometrics 197, 284–297.

Jacod, J., Protter, P., 2012. Discretization of Processes. Springer-Verlag, Berlin. [1521, 1524, 1529, 1530, 1543, 1545-1547].

Jacod, J., Todorov, V., 2009. Testing for common arrivals of jumps for discretely observed multidimensional processes. The Annals of Statistics 37, 1792–1838.

Jacod, J., Todorov, V., 2010. Do price and volatility jump together? The Annals of Applied Probability 20, 1425–1469.

Jing, B.Y., Kong, X.B., Liu, Z., Mykland, P., 2012. On the jump activity index for semimartingales. Journal of Econometrics 166, 213–223.

Joyce, M., Miles, D., Scott, A., Vayanos, D., 2012. Quantitative easing and unconventional monetary policy — An introduction. The Economic Journal 122, F271–F288.

Joyce, M.A.S., Lasaosa, A., Stevens, I., Tong, M., 2011. The financial market impact of quantitative easing in the United Kingdom. International Journal of Central Banking 7, 113–161.

Kapetanios, G., Mumtaz, H., Stevens, I., Theodoridis, K., 2012. Assessing the economy-wide effects of quantitative easing. The Economic Journal 122, F316–F347.

Lahaye, J., Laurent, S., Neely, C.J., 2011. Jumps, cojumps and macro announcements. Journal of Applied Econometrics 26, 893–921.

Lee, S.S., 2012. Jumps and information flow in financial markets. The Review of Financial Studies 25, 439–479.

Lee, S.S., Hannig, J., 2010. Detecting jumps from Lévy jump diffusion processes. Journal of Financial Economics 96, 271–290.

Lee, S.S., Mykland, P.A., 2008. Jumps in financial markets: A new nonparametric test and jump dynamics. Review of Financial Studies 21, 2535–2563.

Lucca, D.O., Moench, E., 2015. The pre-FOMC announcement drift. The Journal of Finance 70, 329–371.

Maneesoonthorn, W., Martin, G.M., Forbes, C.S., 2020. High-frequency jump tests: Which test should we use? Journal of Econometrics 219, 478–487.

Merton, R.C., 1976. Option pricing when underlying stock returns are discontinuous. Journal of Financial Economics 3, 125–144.

Nakamura, E., Steinsson, J., 2018. High frequency identification of monetary non-neutrality: The information effect. The Quarterly Journal of Economics 133, 1283–1330.

Neely, C.J., 2015. Unconventional monetary policy had large international effects. Journal of Banking and Finance 52, 101–111.

Pelger, M., 2020. Understanding systematic risk: A high-frequency approach. The Journal of Finance 75, 2179–2220.

Rodnyansky, A., Darmouni, O.M., 2017. The effects of quantitative easing on bank lending behavior. The Review of Financial Studies 30, 3858–87.

Romano, J.P., Wolf, M., 2005. Stepwise multiple testing as formalized data snooping. Econometrica 73, 1237–1282.

Todorov, V., Bollerslev, T., 2010. Jumps and betas: A new framework for disentangling and estimating systematic risks. Journal of Econometrics 157, 220–235.

Todorov, V., Tauchen, G., 2011. Volatility jumps. Journal of Business and Economic Statistics 29, 356–371.

Todorov, V., Zhang, Y., 2022. Information gains from using short-dated options for measuring and forecasting volatility. Journal of Applied Econometrics 37, 368–391.

Van Oordt, M., Zhou, C., 2016. Systematic tail risk. Journal of Financial and Quantitative Analysis 51, 685–705.

Weller, B.M., 2019. Measuring tail risks at high frequency. The Review of Financial Studies 32, 3571–3616.

Winkelmann, L., Bibinger, T., Linzert, T., 2016. ECB monetary policy surprises: identification through cojumps in interest rates. Journal of Applied Econometrics 31, 613–629.

Wright, J.H., 2012. What does monetary policy do to long-term interest rates at the zero lower bound? The Economic Journal 122, F447–F466.

Supplementary Online Appendix to

"Testing for Multi-Asset Systemic Tail Risk"

This supplementary document contains the appendices that present the technical results, proofs, additional simulation assessments, and various empirical extensions.

Appendices

A Proofs

Remarks and Main Assumptions

Remark 1 (Grigelionis decomposition)**.** *We follow Erdemlioglu and Yang (2022) and consider that X (Equation 1) is an Ito semimartingale taking the form,*

$$X_t = X_0 + \int_0^t b_s ds + \int_0^t \sigma_s dW_s + x * (\mu_t - \nu_t) + (x - h(x)) * \mu_t, \tag{A.1}$$

where the drift term $b = (b_t)$ and the volatility component $\sigma = (\sigma_t)$ are locally bounded, W is a standard Brownian motion, μ is the jump measure of X and ν is its jump compensator. This representation is simply the N-dimensional extension of the univariate and bivariate forms considered in Boswijk et al. (2018) and Dungey et al. (2018), respectively.

Assumption 1. *As in Erdemlioglu and Yang (2022), we assume that ν has the following decomposition*

$$\nu_t(dt, dx) = F_t(x)dt.$$

The predictable random measure F_t has two parts:

$$F_t(dx) = f_t(x)\, \lambda_{t-}\, dx, \tag{A.2}$$

where the predictable function $f_t(x)$ controls the jump size distribution and $\lambda_- = (\lambda_{t-})$ is the stochastic jump intensity that has the following representation:

$$\lambda_t = \lambda_0 + \int_0^t b'_s ds + \int_0^t \sigma'_s dW_s + \int_0^t \sigma''_s dB_s + \delta' * \mu_t + \delta'' * \mu_t^{\perp}, \tag{A.3}$$

where B is a standard Brownian motion independent of W, $\mu_t^{\perp}$ is orthogonal to μ_t, and δ', δ'' are predictable.

Assumption 2. *We follow Erdemlioglu and Yang (2022) and assume that the drift and volatility processes b_t and σ_t in* (A.3) *are locally bounded. There are three (nonrandom) numbers $\beta \in (0,2)$, $\beta' \in [0,\beta)$ and $\gamma > 0$, and a locally bounded process $L_t \geq 1$, such that, for all (ω, t),*

$$F_t = F'_t + F''_t, \tag{A.4}$$

where

(a) $F'_t(dx) = f_t(x)\lambda_{t-}dx$ with $\lambda = (\lambda_t)$ given by (A.3)*, $\lambda_t \leq L_t$ and*

$$f_t(x) = \frac{1 + |x|^\gamma h(t,x)}{|x|^{1+\beta}}, \tag{A.5}$$

for some predictable function $h(t,x)$, satisfying

$$1 + |x|^\gamma h(t,x) \geq 0, \quad |h(t,x)| \leq L_t. \tag{A.6}$$

(b) F''_t is a measure that is singular with respect to F'_t and satisfies

$$\int_{\mathbb{R}} (|x|^{\beta'} \wedge 1) F''_t(dx) \leq L_t. \tag{A.7}$$

Assumption 3. *The function $g(\cdot)$ needs to satisfy the condition*

(i) $g(x) = |x|^p$ if $|x| \leq a$ for some constant $a > 0$ and even integer $p > 2$, and further $g(x)$ is considered even, non-negative, bounded and smooth with a bounded and Lipschitz-continuous first-order derivative. The following forms can then be taken:

$$g_1(x) = \begin{cases} |x|^p & |x| \leq 1, \\ 1 & |x| > 1, \end{cases}$$

for an even integer $p > 2$ and ($x := |\Delta_j^n X|/\alpha\Delta_n^{\varpi}$). Alternatively,

$$g_2(x) = \begin{cases} c^{-1}|x|^p & |x| \leq a, \\ c^{-1}(a^p + \frac{pa^{p-1}}{2(b-a)}((b-a)^2 - (|x|-b)^2)) & a \leq |x| \leq b, \\ 1 & |x| > b, \end{cases}$$

where $0 < a < b < \infty$ and $c = a^p + pa^{p-1}(b-a)/2$.

A.1 Proof of Theorem 1

Proof. According to Theorem 3.1 of Romano and Wolf (2005), we only need to prove that the distributions of

$$\sqrt{\frac{k_n^\lambda \Delta_n}{\Delta_n^{\varpi\widehat{\beta}}}} \left(\widehat{\lambda}(\widehat{\beta}, k_n^\lambda)_t^* - \widehat{\lambda}(\widehat{\beta}, k_n^\lambda)_t \right) \text{ and } \sqrt{\frac{k_n^\lambda \Delta_n}{\Delta_n^{\varpi\widehat{\beta}}}} \left(\widehat{\lambda}(\widehat{\beta}, k_n^\lambda)_{t+} - \lambda_{t+} \right)$$

are asymptotically the same, which is the key assumption (i.e., Assumption 3.1) therein. Note that the proof of the pre-event case is essentially the same.

Let $\mathbb{P}^*$ be the bootstrap probability measure, which assigns equal probability to the k_n^* number of local observations, and $\mathbb{E}^*$ be the expectation under $\mathbb{P}^*$. Furthermore, denote by $\widehat{\lambda}(\widehat{\beta}, k_n^\lambda)_t^*$ the bootstrapped estimate, which is given by

$$\widehat{\lambda}(\widehat{\beta}, k_n^\lambda)_t^* = \frac{\Delta_n^{\varpi\widehat{\beta}}}{k_n^\lambda \Delta_n} \sum_{j \in I_{\lambda,t}^+} \frac{\alpha^\beta}{C_\beta(1)} g_n(\Delta_j^n X^*),$$

where $\Delta_j^n X^*$ is the bootstrapped increments.

According to the bootstrap algorithm, it is easy to see that, for $j \in I_{\lambda,t}^+$, we have

$$\Delta_n^{\varpi\widehat{\beta}-1} \frac{\alpha^\beta}{C_\beta(1)} \mathbb{E}^*[g_n(\Delta_j^n X^*)] = \frac{\Delta_n^{\varpi\widehat{\beta}}}{k_n^\lambda \Delta_n} \sum_{j \in I_{\lambda,t}^+} \frac{\alpha^\beta}{C_\beta(1)} g_n(\Delta_j^n X) = \widehat{\lambda}(\widehat{\beta}, k_n^\lambda)_t.$$

For notation simplicity, let

$$Z_j^* = \sqrt{\Delta_n^{\varpi\widehat{\beta}-1}} \frac{\alpha^\beta}{C_\beta(1)} g_n(\Delta_j^n X^*).$$

Then, we can obtain

$$\sqrt{\frac{k_n^\lambda \Delta_n}{\Delta_n^{\varpi\widehat{\beta}}}} \left(\widehat{\lambda}(\widehat{\beta}, k_n^\lambda)_t^* - \widehat{\lambda}(\widehat{\beta}, k_n^\lambda)_t \right) = \frac{1}{\sqrt{k_n^\lambda}} \sum_{j \in I_{\lambda,t}^+} \big(Z_j^* - \mathbb{E}^*(Z_j^*) \big).$$

Under the bootstrap probability measure, the sequence $\{Z_j^* - \mathbb{E}^*(Z_j^*)\}_{j \in I_{\lambda,t}^+}$ is independent and identically distributed. The variance of Z_j^* under the bootstrap measure $\mathbb{P}$ is given by

$$\begin{aligned}
\mathrm{Var}^*(Z_j^*) &= \mathbb{E}^*[(Z_j^*)^2] - \big(\mathbb{E}^*[Z_j^*]\big)^2 \\
&= \frac{\Delta_n^{\varpi\widehat{\beta}}}{k_n^\lambda \Delta_n} \frac{\alpha^{2\beta}}{[C_\beta(1)]^2} \sum_{j \in I_{\lambda,t}^+} [g_n(\Delta_j^n X)]^2 - \Delta_n^{1-\varpi\widehat{\beta}} [\widehat{\lambda}(\widehat{\beta}, k_n^\lambda)_t]^2 \\
&= \frac{\Delta_n^{\varpi\widehat{\beta}}}{k_n^\lambda \Delta_n} \frac{\alpha^{2\widehat{\beta}}}{[C_{\widehat{\beta}}(1)]^2} \sum_{j \in I_{\lambda,t}^+} [g_n(\Delta_j^n X)]^2 - o_{\mathbb{P}}(1) \xrightarrow{\mathbb{P}} \frac{\alpha^{2\beta} C_\beta(2)}{[C_\beta(1)]^2} \lambda_{t+},
\end{aligned}$$

where the last line follows from the proof of Boswijk et al. (2018), by treating g_n^2 as the function g_n therein.

It then follows that

$$\frac{1}{\sqrt{k_n^\lambda}} \sum_{j \in I_{\lambda,t}^+} \big(Z_j^* - \mathbb{E}^*(Z_j^*) \big) \xrightarrow{L^*} N\big(0, V^*\big).$$

The limiting variance is given by

$$V^* = \mathrm{Var}^*(Z_j^*) \xrightarrow{\mathbb{P}} \lambda_{t+}\alpha^\beta \frac{C_\beta(2)}{[C_\beta(1)]^2}.$$

Therefore, the desired result readily follows. □

A.2 Proof of Theorem 2

Proof. Under $\mathbb{P}^*$, the resampled increments $\{\Delta_j^n X^*\}$ are i.i.d. Define:

$$Z_j^* = \sqrt{\Delta_n^{\varpi\beta-1}} \frac{\alpha^\beta}{C_\beta(1)} g_n(\Delta_j^n X^*).$$

The bootstrap variance is:

$$\mathrm{Var}^*(Z_j^*) = \frac{\Delta_n^{\varpi\beta}}{k_n^\lambda \Delta_n} \frac{\alpha^{2\beta}}{[C_\beta(1)]^2} \sum_{j \in I_{\lambda,t}^+} g_n^2(\Delta_j^n X) - \Delta_n^{1-\varpi\beta}[\widehat{\lambda}_t]^2 \xrightarrow{\mathbb{P}} \lambda_{t+} \frac{\alpha^{2\beta} C_\beta(2)}{[C_\beta(1)]^2}.$$

Since $g_n(x)$ is bounded (Assumption 3), $|Z_j^*| \leq \sqrt{\Delta_n^{\varpi\beta-1}} \cdot C$. As $\sqrt{\Delta_n^{\varpi\beta-1}} \to 0$, the Lindeberg term vanishes.

By the Lindeberg-Feller CLT:

$$\frac{1}{\sqrt{k_n^\lambda}} \sum_{j \in I_{\lambda,t}^+} \left(Z_j^* - \mathbb{E}^* Z_j^*\right) \xrightarrow{L^*} N\left(0, \lambda_{t+} \frac{\alpha^{2\beta} C_\beta(2)}{[C_\beta(1)]^2}\right).$$

□

A.3 Proof of Theorem 3

Proof. Divide the local window $I_{\lambda,t}^+$ into $B_n = \lfloor k_n^\lambda / \ell_n \rfloor$ blocks of length $\ell_n = o(k_n^\lambda)$. Resample entire blocks of increments $\{\Delta_j^n X\}_{j \in \text{block}}$ across all assets to preserve cross-sectional dependence during systemic events.

Under (A4)–(A5), the estimator decomposes as $\widehat{\lambda}_t = \widehat{\lambda}_t^{\text{idiosyncratic}} + \widehat{\lambda}_t^{\text{systemic}}$. By orthogonality,

$$\mathrm{Var}^*(\widehat{\lambda}_t^*) = \mathrm{Var}^*(\widehat{\lambda}_t^{\text{idiosyncratic},*}) + \mathrm{Var}^*(\widehat{\lambda}_t^{\text{systemic},*}) + o_{\mathbb{P}}(1).$$

Apply Theorem 2 to $\widehat{\lambda}_t^{\text{idiosyncratic},*}$:

$$\sqrt{\frac{k_n^\lambda \Delta_n}{\Delta_n^{\varpi\beta}}} \left(\widehat{\lambda}_t^{\text{idiosyncratic},*} - \widehat{\lambda}_t^{\text{idiosyncratic}}\right) \xrightarrow{L^*} N\left(0, \lambda_t^{\text{idiosyncratic}} \frac{\alpha^{2\beta} C_\beta(2)}{[C_\beta(1)]^2}\right).$$

The systemic terms $\{Z_{j,\text{systemic}}^*\}$ form a mixingale sequence with $\alpha(m) = O(m^{-a})$. The Lindeberg-

Feller CLT gives:

$$\sqrt{\frac{k_n^\lambda \Delta_n}{\Delta_n^{\varpi\beta}}}\left(\widehat{\lambda}_t^{\text{systemic},*} - \widehat{\lambda}_t^{\text{systemic}}\right) \xrightarrow{L^*} N\left(0, \lambda_t^{\text{systemic}} \frac{\alpha^{2\beta} C_\beta(2)}{[C_\beta(1)]^2}\right).$$

By Slutsky's theorem and orthogonality (A5), the result follows. □

A.4 Proof of Theorem 4

Proof. We start by showing that truncation eliminates volatility jumps. That is, volatility jumps in (D.9) generate log-return increments over Δ_n of magnitude:

$$\Delta_j^n X_i^{\text{vol}} = \theta 1_{\{S=JT\}} \sqrt{\Delta_n}.$$

Under assumption (i) ($\theta = O(\Delta_n^{1/2})$), the jump size satisfies:

$$|\Delta_j^n X_i^{\text{vol}}| \leq C\Delta_n^{1/2} \cdot \sqrt{\Delta_n} = C\Delta_n.$$

The truncation threshold $\alpha\Delta_n^\omega$ (with $\omega \in (0, 1/2)$) asymptotically dominates Δ_n:

$$\Delta_n \ll \alpha\Delta_n^\omega \quad \text{for small } \Delta_n \implies |\Delta_j^n X_i^{\text{vol}}| < \alpha\Delta_n^\omega.$$

By Assumption 3, $g_n(\Delta_j^n X_i^{\text{vol}}) = 0$, so volatility jumps are excluded from the intensity estimator:

$$\widehat{\lambda}_i^{\text{pre/post}} = \frac{\Delta_n^{\varpi\beta}}{k_n^\lambda \Delta_n} \sum_{j \in I_{\lambda,t}^+} \frac{\alpha^\beta}{C_\beta(1)} g_n(\Delta_j^n X_i).$$

Divide the local window $I_{\lambda,t}^+$ into $B_n = \lfloor k_n^\lambda / \ell_n \rfloor$ blocks of length $\ell_n = o(\Delta_n^{-1/2})$. Resample blocks to preserve dependence within event windows.

By Jacod and Protter (2012) (Theorem 2.3.1), the bootstrap statistic:

$$\mathcal{T}_{i,t}^{(\text{event}),*} = \sqrt{\frac{k_n^\lambda \Delta_n}{\Delta_n^{\varpi\beta}}}\left(\widehat{\lambda}_i^{\text{post},*} - \widehat{\lambda}_i^{\text{pre},*}\right),$$

converges stably in law to the same limit as $\mathcal{T}_{i,t}^{(\text{event})}$. This holds because (1) volatility jumps are truncated (Step 1) and (2) Block length $\ell_n = o(\Delta_n^{-1/2})$ ensures dependence dissipates asymptotically.

For any Lipschitz function f,

$$\mathbb{E}^*\left[f\left(\max_i \mathcal{T}_{i,t}^{(\text{event}),*}\right)\right] - \mathbb{E}\left[f\left(\max_i \mathcal{T}_{i,t}^{(\text{event})}\right)\right] \xrightarrow{\mathbb{P}} 0,$$

by the coupling argument in Jacod and Protter (2012) (Corollary 3.4). Thus,

$$\sup_x \left| \mathbb{P}^* \left(\max_i \mathcal{T}_{i,t}^{(\text{event}),*} \leq x \right) - \mathbb{P} \left(\max_i \mathcal{T}_{i,t}^{(\text{event})} \leq x \right) \right| \xrightarrow{\mathbb{P}} 0.$$

The test statistic $\mathcal{T}_{i,t}^{(\text{event})}$ isolates jumps in $\lambda_{i,t}$ because:

- Diffusion component: $dX_{i,t} = \sigma_{i,t} dW_{i,t}$ is truncated by $g_n(x)$.

- Volatility jumps: Excluded via Step 1.

- Intensity jumps: Governed by $d\lambda_{i,t}$ in (D.10), which directly affects $\widehat{\lambda}_i^{\text{pre/post}}$.

Under H_0 (no intensity jumps), $\max_i \mathcal{T}_{i,t}^{(\text{event})}$ converges to a Gumbel distribution. Under H_1 (intensity jumps), $\mathcal{T}_{i,t}^{(\text{event})}$ diverges, ensuring detection. Thus, the StepM method controls FWER at level α and detects true cojumps in $\lambda_{i,t}$. □

A.5 Proof of Theorem 5

Proof. Let $c_{1-\alpha}^{\text{marginal}}$ be the $(1-\alpha)$-quantile of the standard normal distribution. For each asset i, under $H_{0,i}$:

$$\mathbb{P}\left(T_{i,t} > c_{1-\alpha}^{\text{marginal}} \mid H_{0,i} \right) = \alpha + o(1).$$

Under weak cross-sectional dependence (A11), the probability of no false rejections is approximately:

$$\mathbb{P}\left(\bigcap_{i=1}^{N} \left\{ T_{i,t} \leq c_{1-\alpha}^{\text{marginal}} \right\} \mid H_0 \right) \approx \prod_{i=1}^{N} \mathbb{P}\left(T_{i,t} \leq c_{1-\alpha}^{\text{marginal}} \mid H_{0,i} \right) = (1-\alpha)^N.$$

As $N \to \infty$, $(1-\alpha)^N \to 0$. Thus,

$$\mathbb{P}\left(\text{Reject } H_{0,i} \text{ for some } i \mid H_0 \right) = 1 - (1-\alpha)^N \to 1.$$

The StepM critical value $\widehat{c}_{1-\alpha}^*$ estimates the $(1-\alpha)$-quantile of $\max_{1 \leq i \leq N} T_{i,t}^*$ under the bootstrap measure $\mathbb{P}^*$. By (A12),

$$\widehat{c}_{1-\alpha}^* \xrightarrow{\mathbb{P}} c_{1-\alpha}^{\max}, \quad \text{where } \mathbb{P}\left(\max_{1 \leq i \leq N} T_{i,t} \leq c_{1-\alpha}^{\max} \mid H_0 \right) = 1 - \alpha.$$

Using $\widehat{c}_{1-\alpha}^*$ as the critical value:

$$\mathbb{P}\left(\text{Reject any } H_{0,i} \mid H_0 \right) = \mathbb{P}\left(\max_{1 \leq i \leq N} T_{i,t} > \widehat{c}_{1-\alpha}^* \mid H_0 \right).$$

By the bootstrap validity (A12),

$$\mathbb{P}\left(\max_{1 \leq i \leq N} T_{i,t} > \widehat{c}_{1-\alpha}^* \mid H_0 \right) = \alpha + o_{\mathbb{P}}(1).$$

Thus,

$$\limsup_{N\to\infty} \mathbb{P}\left(\text{Reject any } H_{0,i} \mid H_0\right) \leq \alpha. \qquad \square$$

B Motivating Examples and Schematic Representation

To describe our detection mechanism in mind, let us provide a schematic diagram (Figure S.5) that presents a system-wise representation. The idea is as follows. Suppose that we have N financial assets (Asset 1, Asset 2, ..., Asset N) (i.e., the horizontal axes in the figure). Let us consider that investors and traders closely monitor market developments, they enter the market particularly in periods of important information events (e.g., FOMC news, macro news, earning announcements). The investor can trace a certain category of scheduled news events (E), such as FOMC press release events, denoted by category m. The vertical axis of the figure displays the intradaily arrival times of all FOMC news events over the horizon $[0, T]$, which we fully synchronize across all assets. For each event time ($E^m_{s=1}$,$E^m_{s=2}$,...,$E^m_{s=S}$), we take the testing time points (empty blue circles) and rely on the corresponding pre-/post-event windows (dashed red rectangles) to design our formal tests and associated inference. We do so by looking at the simultaneous (hence systemic) sudden ups-and-downs: we are interested in figuring out which assets cojump together in response to events, when and how frequently we observe these patterns in the data.

To motivate the practical usefulness of this mechanism, we take three systemically important news events: (i) FOMC announcement on interest rate cut (2:15 p.m. EST on December 11, 2007), (ii) the bailout decision news of the U.S. House of Representatives (1:40 p.m. EDT on September 29, 2008) and (iii) the flash crash of May 6, 2010 (also known as *the crash of 2:45 p.m.*).[28] In this particular example with three events, we can test for systemic cojumps conditional on only one event (i.e., $S = 1$), two events (i.e., $S = 2$), or alternatively, by combining all events (i.e., $S = 3$).

We take these three events and apply our procedure to a panel of twenty-two individual Dow Jones stocks (i.e., $N = 22$) and nine Sector ETFs (i.e., $N = 9$). The results (unreported for brevity) clearly confirm the fact that these three events are indeed systemically important, as they create systemic cojumps.[29] A soon as the event time arrives, all individual Dow Jones stocks cojump simultaneously within about 15-seconds following the news and the evidence holds also for sector ETFs. It is also worth emphasizing that these event-induced systemic cojumps are downside, very sharp price declines, that is, they are in the form of event-induced sudden crashes.[30] Using our detection approach, we are able to tell how often crashes occur and which specific events trigger their arrivals.

[28] We follow Caporin et al. (2017) and choose this particular FOMC news event. Of course, the flash crash event is an unscheduled event. We use this event only for illustrative purpose in order to highlight the accuracy of our approach in terms of detecting events that result in systemic collapses in the prices of financial assets.

[29] These results are available upon request.

[30] Our systemic crash (SCRA) detection approach directly builds on the systemic cojump (SCOJ) detection. Specifically, while the former utilizes only negative high-frequency returns (before and after the events), the latter takes into account all high-frequency returns in even windows without any sign restriction (negative or positive).

C StepM Method and Computation of Quantiles with Bootstrap

We implement the event-based version of our StepM method by using the following algorithm.

Algorithm 1. Event-Based StepM Method:

1. For each event ($s = 1, \ldots, S$), use high-frequency data to estimate $\widehat{\lambda}_i^{\text{pre}}$ and $\widehat{\lambda}_i^{\text{post}}$ for all assets ($i = 1, \ldots, N$).

2. Compute the test statistic $\mathcal{T}_{i,t}^{(\text{event})}$ in Equation (6) conditional on time (t) of each event ($s = 1, \ldots, S$) for all assets ($i = 1, \ldots, N$). Analogous to Romano and Wolf (2005) (p. 1239 and 1247), the statistic measures the post-event *tail riskiness* of each asset relative to the each asset's benchmark (i.e., pre-event risk). The testing data matrix is $N \times S$.

3. Relabel the assets (for a given event) in descending order of all test statistics $\mathcal{T}_{i,t}^{(\text{event})}$: asset r_1 corresponds to the largest test statistic and asset r_i to the smallest.

4. Set $j = 1$ and $R_0 = 0$ (the number of null hypothesis initially rejected).

5. For $R_{(j-1)} + 1 \leq i \leq N$, if $0 \notin [\mathcal{T}_{r_i,t}^{(\text{event})} - \hat{c}_j, \infty)$, reject the null hypothesis $H_0^{(r_i)}$.

6. (a) If no (further) null hypotheses are rejected, stop.

   (b) Otherwise, denote by R_j the total number of hypotheses rejected so far and, afterward, let $j = j + 1$. Then, return to step 5.

where $\hat{c}_j$ denotes the bootstrapped quantiles that we compute directly from the estimated (probability) distribution under the null.

We describe below the procedure regarding how to compute the $\hat{c}_j$ in Algorithm 1 by using bootstrap.

Algorithm 2. Computation of quantiles:

1. The labels $r_1, \ldots, r_i$ and the numerical values of the number of null hypotheses rejected in each step; R_0, R_1,... are given in Algorithm 1 (main text).

2. Recall there are N assets and S events. Generate $M \geq 1000$ bootstrap $(N \times S)^{*,1}$, ..., $(N \times S)^{*,M}$ data matrices.

3. From each bootstrap data matrix $(N \times S)^{*,m}$, $1 \leq m \leq M$, compute the individual test statistics $\mathcal{T}_{1,t}^{(\text{event}),*,m}$, ..., $\mathcal{T}_{N,t}^{(\text{event}),*,m}$ by using high-frequency data, as described in Algorithm 1.

4. (a) For $1 \leq m \leq M$, compute the maximum of individual differences (between test statistics and true parameter); $\max_j^{*,m} = \max_{R_{j-1}+1 \leq i \leq N} (\mathcal{T}_{r_i,t}^{(\text{event}),*,m} - \theta_{r_i,t}^{(\text{event}),*})$.

   (b) Compute $\hat{c}_j$ as the $1 - \alpha$ empirical quantile of the M values $\max_j^{*,1}$, ..., $\max_j^{*,M}$.

Table S.1: Power of the uncorrected and bias-corrected tests based on StepM

		$S = 1$			$S = 10$		
Panel A.		Uncorr	Step-1	StepM	Uncorr	Step-1	StepM
($N = 200$)	15-sec	99.95%	99.70%	99.95%	99.91%	95.77%	99.61%
	1-min	99.20%	92.15%	96.85%	95.51%	69.53%	73.67%
Panel B.							
($N = 20$)	15-sec	100.00%	99.70%	100.00%	97.37%	74.20%	87.19%
	1-min	98.10%	93.30%	98.20%	97.87%	94.40%	97.54%
Panel C.							
($N = 20$)	15-sec	85.70%	71.20%	76.10%	92.86%	62.52%	79.70%
	1-min	94.50%	82.40%	89.70%	76.94%	34.86%	45.58%

Notes: The table reports the frequency of rejections in the presence of news-driven systemic cojumps. The test statistic that we use in simulations is given by Equation (6) in the main text. We consider three versions of the detection procedure: the uncorrected test without accounting for the multiple test bias (labeled as "Uncorr"), the bias-corrected version based on one-step correction (labeled as "Step-1") and the bias-corrected version based on M-step correction (labeled as "StepM"). We provide the details of the simulation setup and parameter selection in Supplementary Appendix 5. The table presents the simulation results when there is only one event (i.e., $S = 1$) and when there are ten events ($S = 10$). We report the rejection rates for 15-seconds and 1-minute sampling frequencies. We set the jump sizes as $\xi = 100$ in Panels A and B, and $\xi = 50$ in Panel C in order to assess the impact of jump size on detection power.

Table S.2: Macroeconomic news announcements

News type	News ticker	Release time	Frequency	Relevance	Events
GDP Annualized QoQ	CQOQ	8:30	Quarterly	96.81	54
Unemployment Rate	USURTOT	8:30	Monthly	89.28	163
CPI MoM	CPI CHNG	8:30	Monthly	95.41	163
ISM Manufacturing	NAPMPMI	10:00	Monthly	95.83	163
New Home Sales	NHSLTOT	10:00	Monthly	90.44	163

Notes: The table presents the description of the macroeconomic news announcements that we used for the implementation of systemic cojump tests. We obtain the time stamps of all macro news from Bloomberg and follow Cieslak and Schrimpf (2019) to choose the type of our macroeconomic news announcements (see page 302 therein). The table provides the news type (first column), the Bloomberg ticker of the event (second column), the release time (third column), the release frequency (fourth column), Bloomberg relevance scores (fifth column) and the number of news events in our sample (last column). In addition to GDP/Unemployment/Inflation announcements considered in Cieslak and Schrimpf (2019), we also include ISM Manufacturing and New Home Sales, as these type of macro news events have very high Bloomberg relevance scores (90% and above). The sample covers the periods from January 3, 2006 to July 24, 2019.

D Construction of Monetary Policy Shocks

To estimate monetary policy shocks, we take the steps described in Fawley and Neely (2014).

D.1 Target and Path Surprises

Let F denote the unobserved monetary factors, as in Chordia et al. (2005). We identify monetary policy shocks from the model

$$Y = F\Phi + \eta \tag{D.8}$$

where Φ denotes the factor loadings on the variable Y and η is a white noise process. We follow Gürkaynak et al. (2005) and include five variables in Y: (I) the surprise to the federal funds target measured from current-month federal funds futures; (2) the surprise change in expectations of the federal funds target two FOMC meetings ahead; and the price change in (3) 6-month, (4) 9-month, and (5) 12-month eurodollar futures contracts. Note that we measure the surprise component in variable (2) directly from the appropriate fed funds future contract.

The next step is then to construct the target and path factors as a linear transformation of the first two principal components (Z) of Y. That is,

$$F = ZL \tag{D.9}$$

where Z contains the first two principle components of Y, and L is a 2×2 matrix. We identify the elements of L by imposing three restrictions: (1) the columns of L have unit length, (2) the columns of F are orthogonal, and (3) F_2, the second column of F, does not influence the current federal funds shock. The third restriction provides the structural interpretation of F_1 and F_2 as the target and path surprise, respectively. While the target factor F_1 contains all information from the first two principal components, the path factor F_2 accommodates the information in residuals. To ease comparison, when needed, we normalize these two factors.

D.2 Wright (2012) Surprises

We follow Wright (2012) and estimate the third form of monetary shock as the first principal component of high-frequency yield curve changes. We use data on the 2, 5, 10 and 30-year Treasury bond futures prices in 2-hour windows around monetary policy decisions. The windows start 15 minutes before each announcement and end 1 hour and 45 minutes after. It is worth mentioning that this window length is quite compatible with that we use in our detection analysis. As in Wright (2012), we further rescale the principal component and sign shocks so that falling (rising) yields produce positive (negative) shocks.

E Results of Robustness Checks

In this section, we present the results of our robustness checks and additional empirical assessments. We begin by presenting additional results and patterns for sector ETFs (Section E.1). Section E.2 explores

the role of negative versus positive MP shocks in driving the systemic response of markets to FOMC news. In Section E.3, we examine whether macroeconomic news announcements lead to systemic cojumps. We generate heat maps for visualizing the systemic response of assets to macro news and compare the reaction maps with that of FOMC news.

E.1 Additional Results for Sector ETFs

We plot in Figures S.1 and S.2 the pre-/post-FOMC realized volatility and news-driven risk scores for sector ETFs, respectively.

Figure S.1: Pre- and post-FOMC realized volatility of sector ETFs

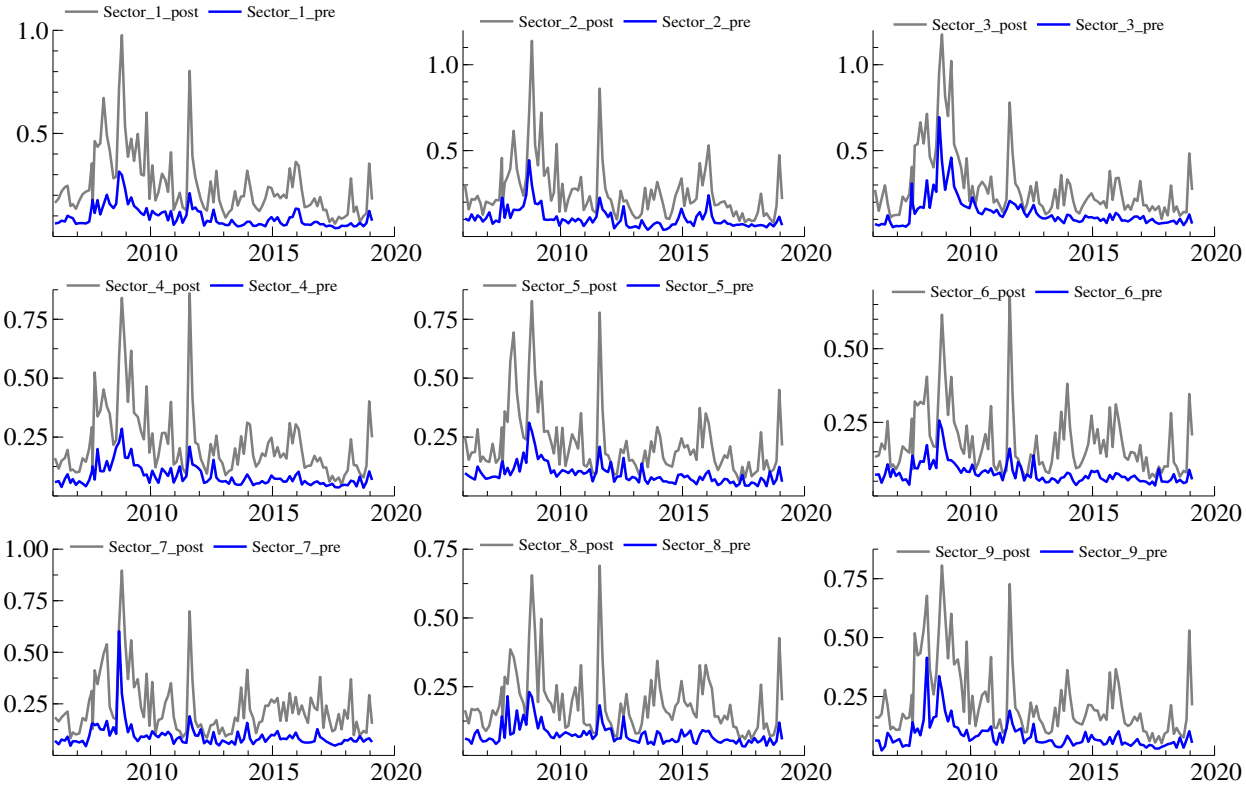

Notes: The figure shows the realized volatility of each sector ETFs, computed before and after the release of each FOMC announcement in the event windows. The dark gray (blue) lines indicate the post-event (pre-event) realized volatility, respectively. The sample covers the periods from January 31, 2006 to January 30, 2019, and contains 106 FOMC policy announcements. Table 1 details the description of each sector ETF that we used in our analysis. The sampling frequency is 15-seconds.

E.2 Negative versus Positive Monetary Policy Shocks

We plot the number Fed-driven systemic cojums in Figure S.3, based on the *most extreme* (i.e., ordered) negative versus positive monetary policy shocks (left versus right panels).

Figure S.2: News-driven tail risk scores computed from standardized test statistics based on sector ETFs

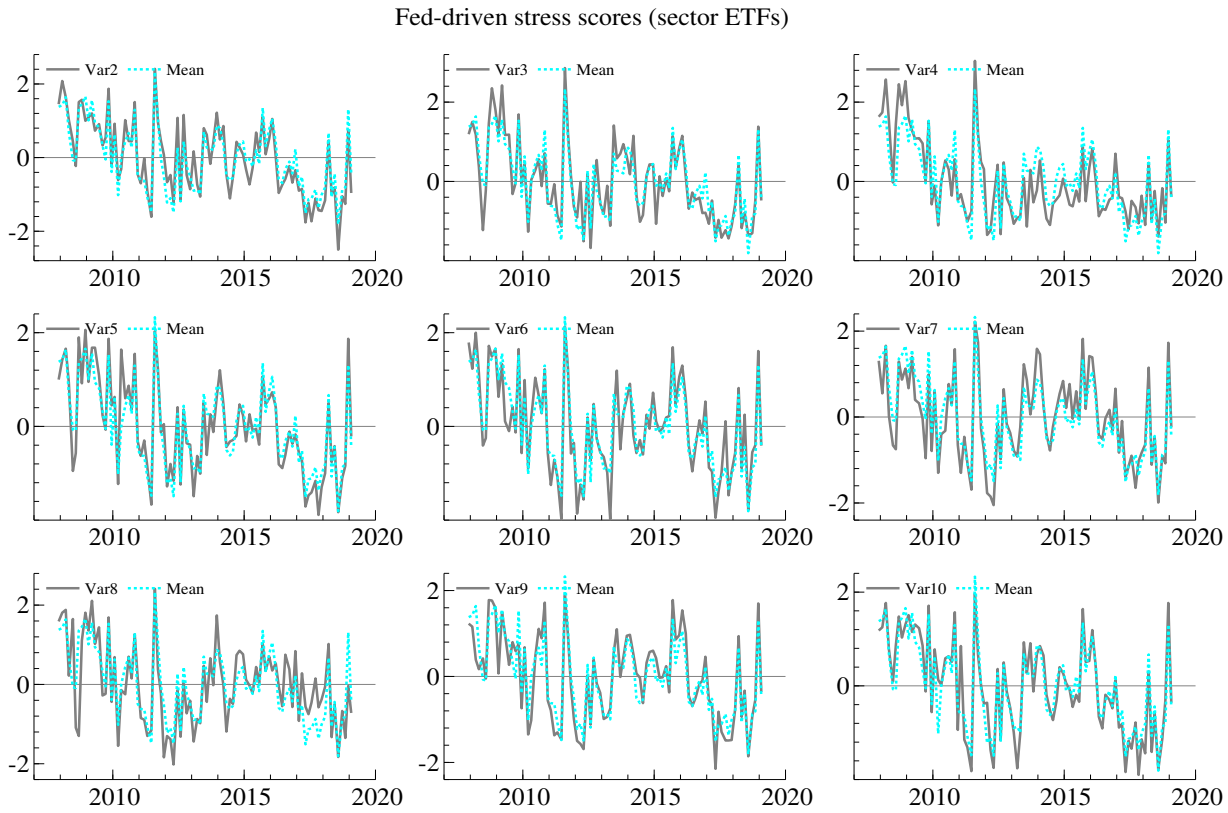

Notes: The figure demonstrates the news-driven realized tail risk (RS) scores of each sector ETF in our sample, compared to cross-sectional average. For each ETF, the RS scores are the values of standardized test statistics that we compute conditional on the release time of each FOMC news announcement. The sample covers the periods from January 31, 2006 to January 30, 2019, and contains 106 FOMC policy announcements. See Figure 1 for the details of the shock estimation approach and target/path/wright factors displayed on the upper panel. Table 1 details the description of each sector ETF that we used in panels. The sampling frequency to compute test statistics is 15-seconds.

Figure S.3: Negative versus positive monetary policy shocks and systemic cojumps of Dow Jones stocks

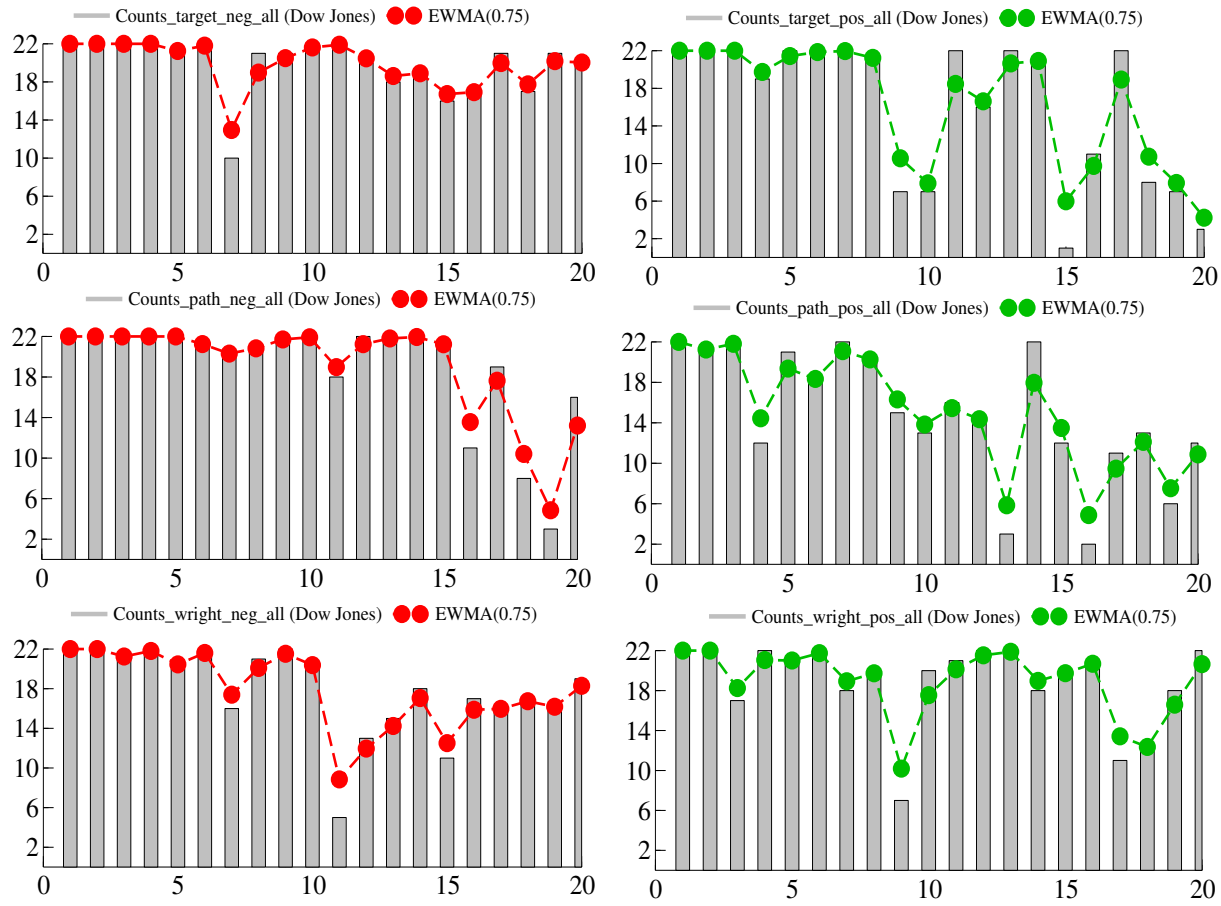

Notes: The figure shows the number of systemic cojumps detected based on the release times of the most surprising FOMC policy decisions. We consider three monetary policy shock factors (target/path/wright) and separate positive shocks from negative shocks. We then apply our testing procedures to only positive shocks (right-panels) and only negative shocks (left-panels) ranked from the largest to smallest. The results are based on the high-frequency data on 22 stocks (X-axis) listed in the Dow Jones index. Table 1 details the description of these Dow Jones stocks. The sampling frequency is 15-seconds. To ease visualization, we display the patterns only for the top 20 news events (Y-axis) yet the full testing results and jump counts are available upon request. The sample covers the periods from January 31, 2006 to January 30, 2019.

E.3 Macroeconomic News Announcements

A natural extension of our study is to explore the link between macroeconomic news announcements and systemic cojumps. This assessment can allow us to evaluate whether or not macro news causes many asset to jump contemporaneously.

Table S.2 provides the description of the macroeconomic news announcements that we use in this analysis. In addition to GDP, Unemployment and Inflation announcements used in Cieslak and Schrimpf (2019), we also include ISM Manufacturing and New Home Sales, as these two announcement types have very high Bloomberg relevance scores (90% and above). To facilitate the evaluation of possible systemic effects, we generate *heat maps* conditional on each macro news for all individual stocks. Figure S.4 displays these systemic reaction maps. The metric on the top-left of each panel further provides the range of the statistics, which helps examine the severity of the tail risk levels conditional on the macro news.

Figure S.4: Systemic reaction heat maps for news announcements

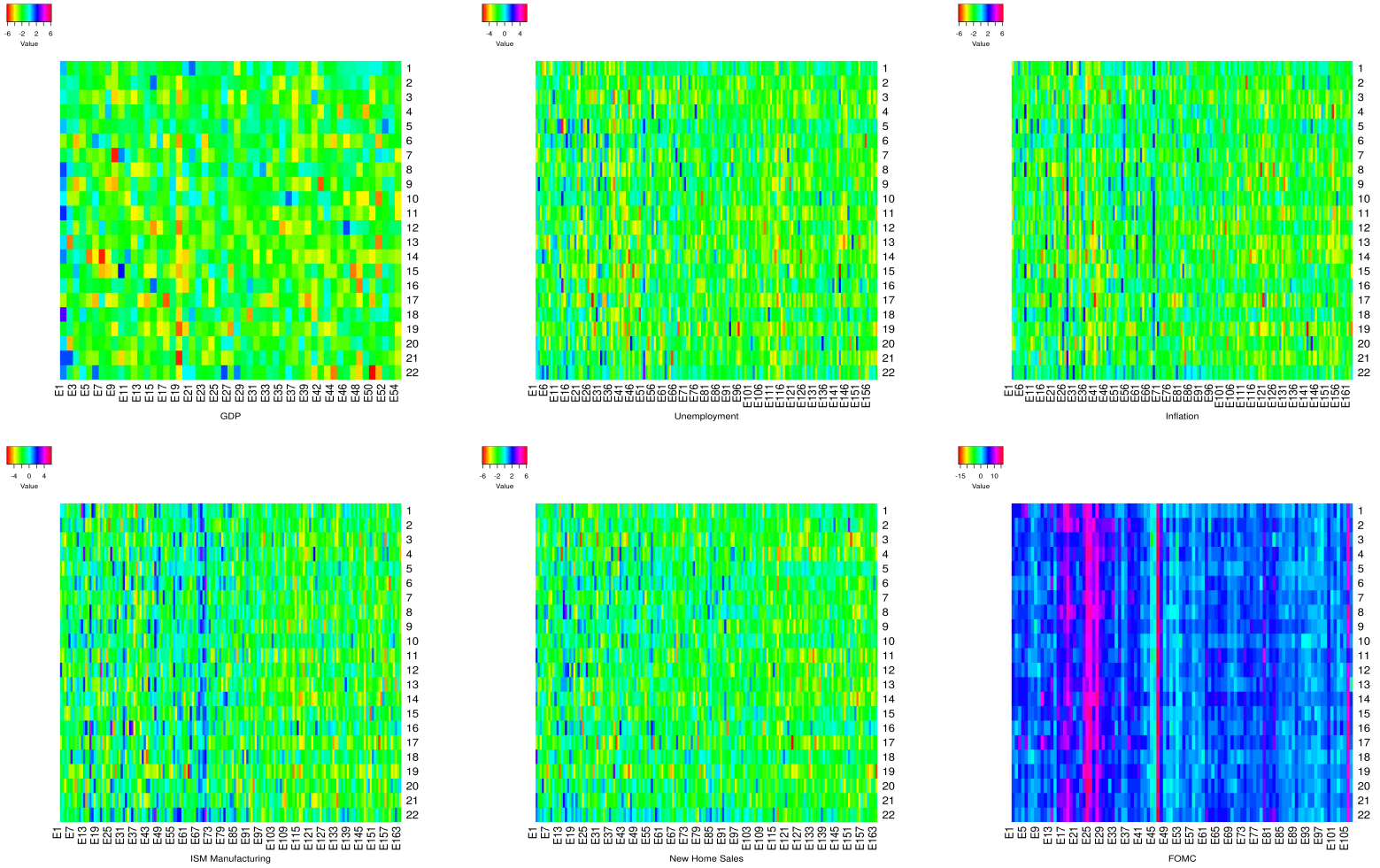

Notes: The figure displays the heat maps of the systemic cojump test statistics conditional on different macroeconomic news announcements. In the upper panels, we construct the maps by computing the test statistics based on the release times of GDP news (left), Unemployment news (middle) and Inflation news (left). In the lower panels, we use ISM Manufacturing announcements (left), New Home Sales announcements (middle) and also FOMC announcements (right) to ease comparison between macro-driven versus Fed-driven systemic responses. In each panel, the X-axis denotes the events and Y-axis indicates the stock. The metric on the top-left of each panel provides the range of the statistics, thereby reflecting the severity of the tail risk levels, given the news event. We obtain the time stamps of all macro news from Bloomberg and follow Cieslak and Schrimpf (2019) to choose the type of our macroeconomic news announcements (see page 302 therein). In addition to GDP/Unemployment/Inflation announcements considered in Cieslak and Schrimpf (2019), we also include ISM Manufacturing and New Home Sales, as these type of macro news events have very high Bloomberg relevance scores (above 90%). The sample covers the periods from January 3, 2006 to July 24, 2019. Table S.2 provides the description of the news announcements and implemented data adjustments.

Figure S.5: Schematic diagram of event-driven systemic cojump and crash testing framework

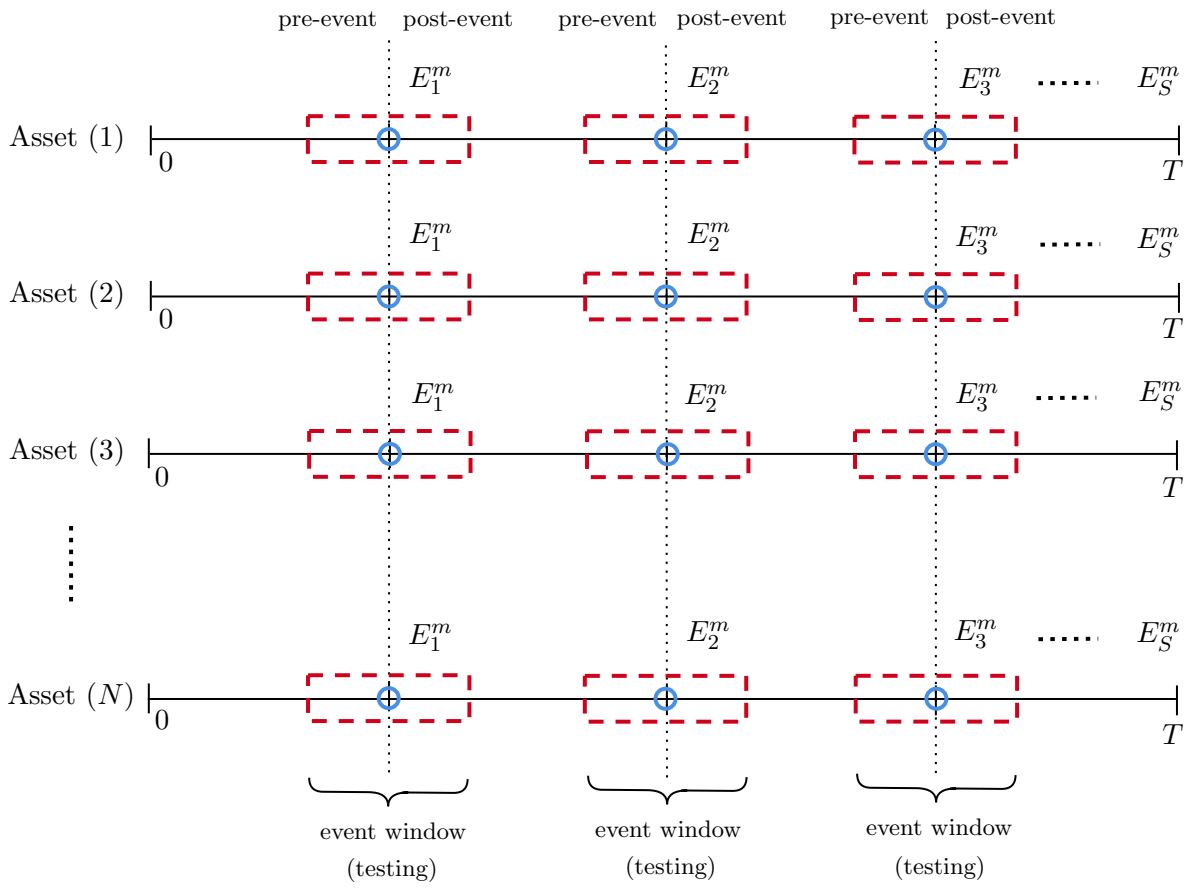

Notes: The figure displays the schematic diagram of the event-based systemic cojump and crash testing approach. We place the N financial assets (1, 2,...,N) horizontally and the arrival times of a certain category of scheduled news events (such as FOMC news with factor classification of "m") are given on vertical axes (i.e., $E^m_{s=1}$,$E^m_{s=2}$,...,$E^m_{s=S}$). For each event, the diagram further indicates the testing time points (empty blue circles), the representative pre-/post-event windows (dashed red rectangles) which we rely on for estimations to detect systemic cojumps. The systemic crash (SCRA) detection approach relies on the systemic cojump (SCOJ) detection. While the former utilizes only negative high-frequency returns before and after the events, the latter takes all high-frequency returns without any sign restriction (i.e., negative or positive). In the diagram, all events arrive over the *global* time horizon (i.e., [0,T]) that represents trading days that we fully synchronize across assets.

E.4 Alternative Tail Risk Measures and Comparison

We compare the ranking of tail risk events identified by our measure with the ranking generated based on the $BT11Q$ approach and measures of (see Bollerslev et al., 2015; Andersen et al., 2021 and Todorov and Zhang, 2022). Table S.3 reports the ranking of the tail risk events.

Table S.3: Ranking of tail risk events identified based on different measures

RANK	TOP TEN (STR)	TOP TEN (LSTR)	TOP TEN (BT11Q)	TOP TEN (LTV)	TOP TEN (VIX)
1	2011-08-09	2011-08-09	2008-10-29	2008-10-29	2008-10-29
2	2008-10-29	2008-10-29	2008-12-16	2008-12-16	2008-12-16
3	2008-12-16	2008-12-16	2011-08-09	2011-11-02	2009-03-18
4	2009-03-18	2009-03-18	2009-01-28	2009-01-28	2009-01-28
5	2009-01-28	2009-01-28	2009-03-18	2009-03-18	2011-09-21
6	2015-09-17	2011-09-21	2011-09-21	2011-08-09	2009-04-29
7	2008-03-18	2015-09-17	2009-04-29	2011-09-21	2011-08-09
8	2009-04-29	2009-04-29	2011-11-02	2009-11-04	2011-11-02
9	2011-09-21	2009-06-24	2009-06-24	2009-08-12	2009-06-24
10	2009-06-24	2016-01-27	2010-06-23	2016-06-15	2009-11-04

Notes: The table presents the ranking of the tail risk events identified based on the proposed systemic tail risk (STR) and systemic left-tail risk (LSTR) measures (second and third columns) versus alternative measures (from fourth column to sixth column). BT11Q is the option-based tail risk measure of Bollerslev and Todorov (2011), LTV denotes the left-tail variation measures developed by Bollerslev et al. (2015); Andersen et al. (2021) and Todorov and Zhang (2022). VIX is the volatility index.

E.5 Empirical Testing Performance: Bias-Corrected Test Versus Basic Test

We compare the systemic cojumps detected by our StepM (bias-corrected) test with those detected by the version without the correction. Table S.4 presents the summary statistics for both tests.

Table S.4: Summary statistics for the bias-corrected versus uncorrected tests

	Bias correction (Dow Jones)	No correction (Dow Jones)	Bias correction (Sector ETFs)	No correction (Sector ETFs)
Mean	12.77	18.61	4.93	6.49
Median	13	21	5.5	8
Std. Deviation	7.76	5.22	3.51	2.92
Sample Variance	60.23	27.21	12.33	8.54
Kurtosis	-1.48	4.02	-1.62	-0.42
Skewness	-0.19	-2.08	-0.20	-0.98
Minimum	0	0	0	0
Maximum	22	22	9	9
Sum (jumps)	1354	1973	523	688
Count (events)	106	106	106	106

Notes: The table reports the summary statistics for the test based on the StepM approach and the test without any correction. The table reports the average number of systemic cojumps detected for a given event (mean), the median, standard deviation, and other descriptive statistics. The table displays the total number of jumps in response to all events (sum (jumps)) for all Dow Jones stocks and Sector ETFs. The "Count (events)" indicates the total number of FOMC events used in the analysis. For further details, see Tables 1 and 2 in the main text.